Torus Immersions and Transformations

Carlo H. Séquin
CS Division, University of California, Berkeley
E-mail: sequin@cs.berkeley.edu

Abstract

All possible immersions of a torus in 3D Euclidean space can be grouped into four regular homotopy classes. All possible immersions within one such class can be transfigured into one another through continuous smooth transformations that will put no tears, creases, or other regions of infinite curvature into the surface. This report introduces four simple, easy-to-understand representatives for these four homotopy classes and describes several transformations that convert a more complex immersion of some torus into one of these representatives. Among them are transformations that turn a torus inside out and others that will rotate its surface parameterization by 90 degrees.

1. Introduction

According to the paper by Hass and Hughes [6], an orientable 2-manifold of genus *g*, immersed in Euclidean 3D space ($\mathbf{R}^3$), has 4^g regular homotopy classes. Surfaces belong to the same class if they can be smoothly transformed into one another without ever experiencing any cuts, or tears, or creases with infinitely sharp curvature; however, the surface is allowed to pass through itself. For genus zero there is only one class. Thus a sphere can be turned inside-out through a sequence of regular homotopy moves. This was first proven by Steve Smale in 1958 [13], but it took many years before a first sequence of actual moves was published [11]. A more elegant sphere-eversion process was later conceived by Bernard Morin [10], and it led to a first computer-graphics movie of that transformation created by Nelson Max [9]. The same basic series of moves was later optimized in the film *Optiverse* [14] so as to minimize the highest level of bending energy reached during that process. Another sphere eversion process relying on *Dirac's Belt Trick* [5] has become well-known through the video *Outside-In* [8].

Based on that same paper [6], we expect four different immersion classes for the torus, where the representatives in one class cannot be turned into that of another class through regular homotopy-preserving moves. Strangely, much less work than for the sphere has been done for the torus to visualize its four regular homotopy classes and possible transformations within them. I could not find any reference that shows representatives of all four classes side by side as in Figure 1. This document tries to fill this void. It is aimed at geometry-minded readers and at the computer-graphics community. For that reason I avoid references to *cohomology classes* and to *group theory*.

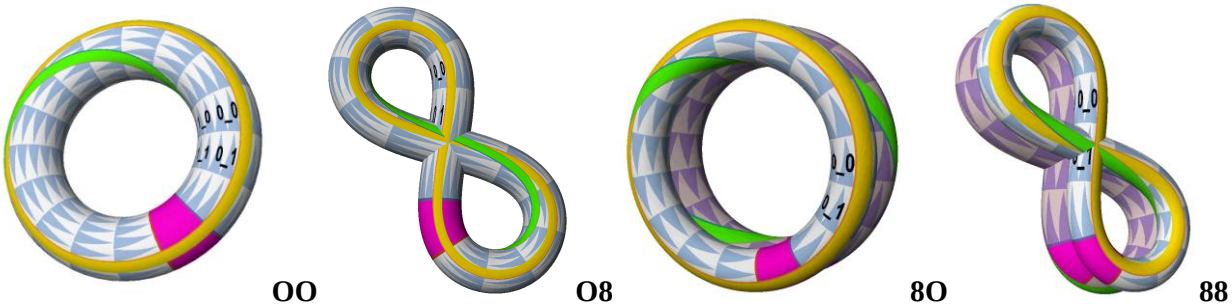

Figure 1: *Tori in four different homotopy classes, characterized by their profile and sweep path (***O****/****8****), with 3 embedded characteristic ribbons: meridians (red), parallels (yellow), (1,1)-diagonals (green):*
Type **OO***: meridians: untwisted, parallels: untwisted, (1,1)-diagonals: 360° twist;*
Type **O8***: meridians: untwisted, parallels: 360° twist, (1,1)-diagonals: untwisted;*
Type **8O***: meridians: 360° twist, parallels: untwisted, (1,1)-diagonals: untwisted;*
Type **88***: meridians: 360° twist, parallels: 360° twist, (1,1)-diagonals: 360° twist.*

2. Torus Parameterization and Nomenclature

Unambiguous naming of the parameter lines on a generalized torus is somewhat tricky. On an ordinary torus of type **OO** (Fig.1a) the lines of curvature provide a natural parameterization grid. However, if the sweep path is not planar, but an arbitrary 3D space curve, the torsion-minimizing parameterization will generally produce "longitudinal" lines (running perpendicularly to the profile curves) that do not close smoothly around the toroid, and which would require some amount of twist (around the sweep path) to keep these lines connected to themselves. In order to clearly define a nomenclature for describing the surface parameterization, the construction of the torus is envisioned as follows: We take a rectangular domain and fold it up onto itself, so that opposite edge pairs merge with proper orientation (Fig.2a). Already the first merger of such an edge pair can be done in many different ways: It may either form a cylindrical tube (Fig.2b), or the rectangle may pass through itself to form a figure-8 shape (Fig.2c) or a cylinder with two or more layers (Fig.2d). The profile curves, lying in planes perpendicular to the cylinder axis, are called *meridians*.

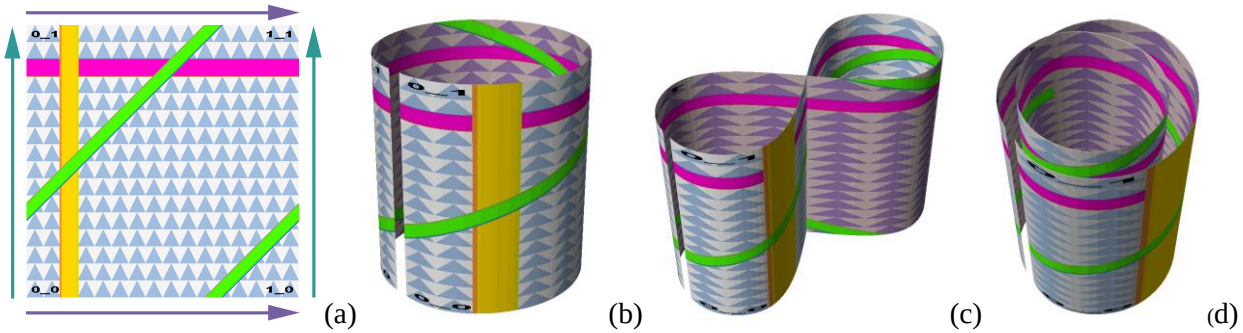

Figure 2: *Step #1 of folding up a rectangular domain (a) into a torus: Merging the two vertical edges: (b) into a cylinder, (c) into a self-intersecting figure-8 shape, or (d) into or a multiply-rolled tube.*

In the second merger step, where these "tubes" are closed into a loop, this closure may be performed without any twist (Fig.3a), or with discrete twists in increments of a full turn (Fig.3b). The sweep path of this loop may be circular (Fig.3a,b), or it may form multiple loops, a self-intersecting figure-8 shape (Fig.3c), or even more complex knots or tangles.

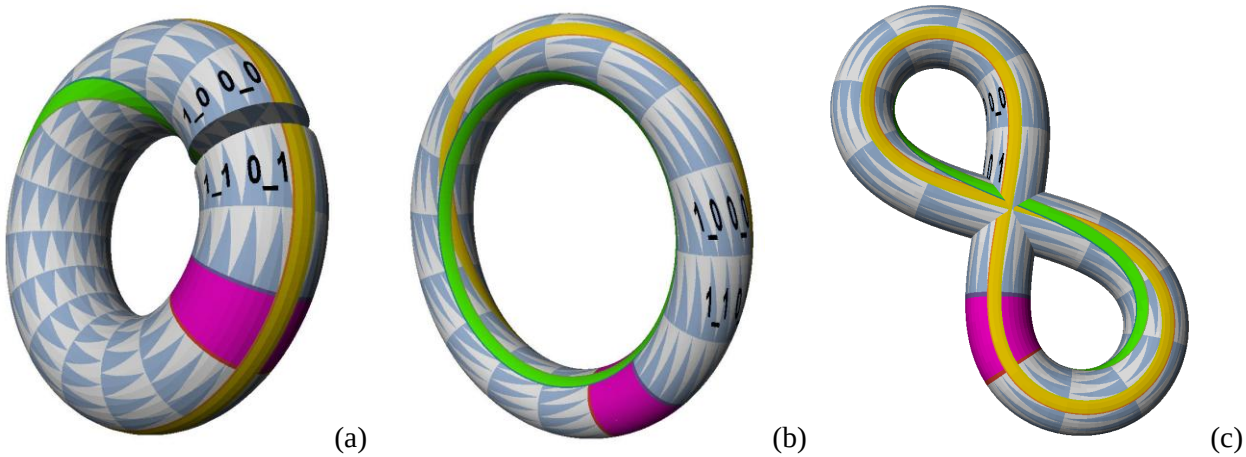

Figure 3: *Step #2 of folding up a rectangular domain into a torus: Merging the horizontal edges to close the tube: (a) on a circular path with no twist, (b) with 360° twist, and (c) along a Figure-8 path.*

To reduce the ambiguity as to how the second set of parameter lines should be drawn, we will use a torus with a **planar sweep path** as a reference. The plane containing that sweep path is called the *equatorial plane*. All meridians then lie in planes that are perpendicular to the equatorial plane. If the cross section is

constant and swept in a torsion minimizing manner, then the second set of parameter lines will lie in planes that are parallel to the equatorial plane, and they can thus naturally be called *parallels*. (Topologists often call these lines "longitudes"; this is unfortunate, because on the globe the lines of longitude are called meridians.) We also call the few special parallels that lie in the equatorial plane *equatorials*. There are also *diagonal* lines that close on themselves. They combine integer numbers of loops along a meridian and along a parallel. On an ordinary torus, a (*1,1)-diagonal* will travel exactly once around the major and minor circles, respectively.

We evaluate the result of this fold-up process not just as an unmarked shape, but as a parameterized surface that displays the parameter markings of the original rectangular domain, the front of which is shown in Figure 2a. The back of this rectangle carries the same (mirrored) pattern but with a more purplish hue and darker shading. We will only allow transformations that maintain the end-to-end connectivity of the pattern placed on this rectangle. In these transformations, surface regions may pass through one another, but no tears, punctures, creases, or spots of infinitely sharp curvature are allowed. At any moment, every small localized piece of the torus surface must be homeomorphic to a disk. If this condition is fulfilled, we call this an *immersion* of the torus in 3D Euclidean space ($\mathbf{R}^3$).

3. Capturing Four Different Representatives

Following a suggestion made in a personal communication by John Sullivan, an easy way to get four distinct representatives of the four regular homotopy classes of the torus is to fold up the two dimensions of the rectangular fundamental domain of the torus surface in either a circular way (**O**) or along a figure-8 path (**8**). This will result in the four classes of tori shown in Figure 1. They can be distinguished unambiguously by the amount of twisting experienced by a pair of complementary ribbons on that surface. Figure 1 shows ribbons along a meridian in magenta (red), ribbons along parallels in yellow, and an additional (1,1)-diagonal ribbon in green. In all four cases the major curve along which a circular or a figure-8 cross section has been swept lies in a plane. Thus when using a torsion-minimizing surface parameterization, all parallels will nicely close on themselves, as well as the three characteristic ribbons.

Some readers may object to the self-intersecting figure-8 sweep paths used in the tori of type **O8** and **88**. We can eliminate the self-intersections at the cross-over points and untangle the figure-8 shape into a perfectly round torus (Fig.4 and 5), but in this process we will introduce ±360° of twist around the sweep path – with the sign depending on the direction in which we move the two crossing branches apart. The result is equivalent to a regular torus on which a Dehn twist [4] along a meridial cut line has been introduced; we thus call this an *M-twist*. In this twisting operation all meridial ribbons (magenta) will remain untwisted.

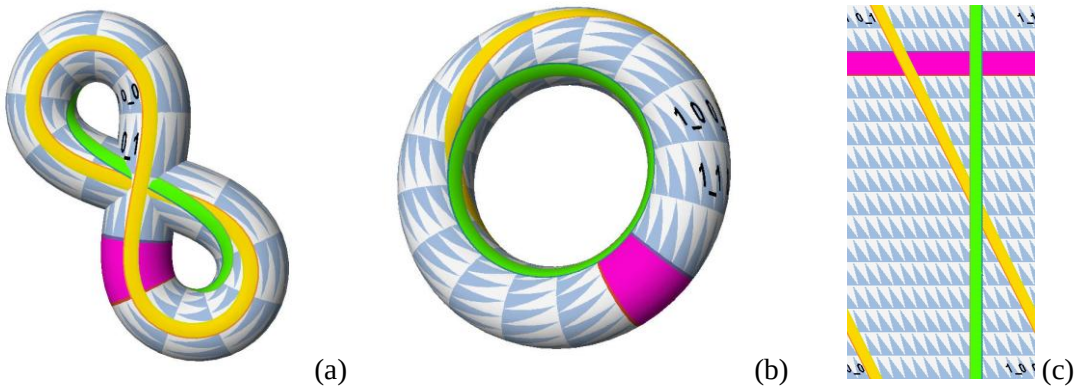

Figure 4: *Untangling the figure-8 path of type* **O8***: (a) incremental* ***down****ward move of torus branch with the green ribbon on top; (b) completed untangling into a torus with twist; (c) unwrapped surface texture.*

In Figure 4b, the green diagonal ribbon has turned into a parallel ribbon, and the yellow ribbon has become a (-1,1)-diagonal. In Figure 5, we separate the crossing torus branches in the opposite directions, and the yellow ribbon becomes a (1,1)-diagonal, while the green ribbon now becomes a (2,1)-diagonal, which shows up on the torus surface as a (1,2)-torus knot with a total twist of the corresponding ribbon of 720°. The readers are encouraged to take a long, thin, physical paper strip, to model it in the shape of any of the above colored surface ribbons, and then to verify the amount of twisting found in the ribbon.

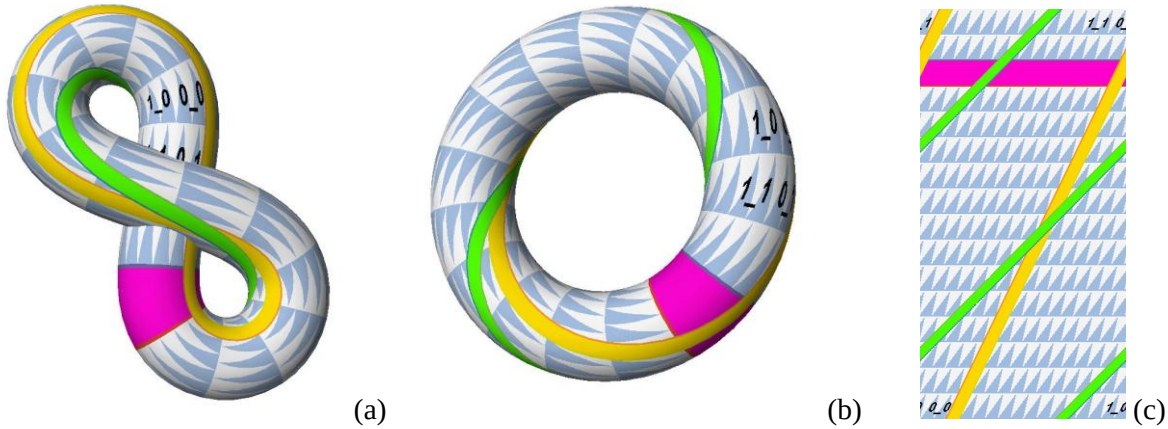

Figure 5: *Different untangling of type* **O8***: (a) incremental* ***up****ward move of the branch with the green ribbon on top; (b) completed untangling into a torus with twist; (c) unwrapped surface texture.*

Figure-8 Cross-Over Move

By going through the regular homotopy transformation starting from Fig.4b through Fig.4a and Fig.5a to Fig.5b we have changed the (meridial) twist in the toroidal loop by 720° while remaining in the same regular homotopy class. We call this whole sequence of transformations a *Figure-8 Sweep Cross-over Move* (F8SwXo-move). By repeating or reversing this move, we can always add or subtract meridial twist in increments of 720°. Thus for our classification of torus immersions, we will count twists modulo 720°.

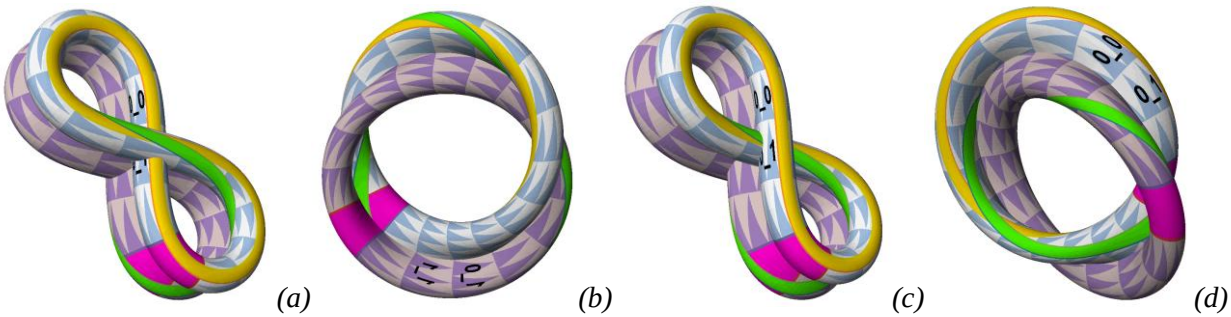

Figure 6: *Untangling the figure-8 path of Type* **88***: (a→ b) result of moving the green-yellow crossing* ***up****wards; (c→ d) result of moving the green-yellow ribbon-crossing* ***down****wards.*

The F8SwXo-move can also be used to untangle the central crossing in tori of type **88** (Fig.6a). Again, depending on the way in which the crossing strands are moved apart in order to separate them, when the figure-8 path has been unwound into a planar, circular loop, a twist of ±360° will have been introduced. For this surface the difference between a negative twist (Fig.6b) and a positive twist (Fig.6c) is much more obvious, since it shows up in the surface geometry itself, and not just in its parameterization. The moves leading from Figure 6a to either Figure 6b or 6c will be called *UtF8Sw* ("Untangle Figure-8 Sweep") and their inverses *CrF8Sw* ("Create Figure-8 Sweep"). The combination CrF8Sw + UtF8Sw

then is equivalent to a F8SwXO-move, resulting in a total twist of 720°. As a preview of what will become clear later in this report: If we do not pay attention to the parameterization of the torus surface, the tori of types **OO**, **O8**, and **8O** are all in the same homotopy class, but the torus of type **88** (Fig.6) is in a class of its own.

4. Another Set of Representatives

Matthias Goerner introduced me to a different way of finding four distinct representatives for the four regular homotopy classes of the torus: One is just the regular torus of type **OO** shown in Figure 1a. To find three other ones, we take the three curves along which we had generated the colored ribbons in Figure 1, and for each one in turn we reshape the torus surface into a small sharp cusp along that line, as shown for a meridial line in Figure 7a. Along that line we then sweep a "drop"-shaped cross section (Fig.7b) and fuse the old and the additional surface along that cusp line into a self-intersecting surface. If the cusp line is a parallel (yellow ribbon), we clearly obtain a torus of type **8O** (Fig.1c). If we use the diagonal line that generated the green ribbon, we obtain type **88** (Fig.6b). But if we choose the red meridial cusp line (Fig.7a), we obtain an interesting new shape (Fig.7c). Since all four representatives are supposed to be different, this last shape (Fig.7c) must be of type **O8**, and there must exist a smooth transformation that converts these two shapes into one another.

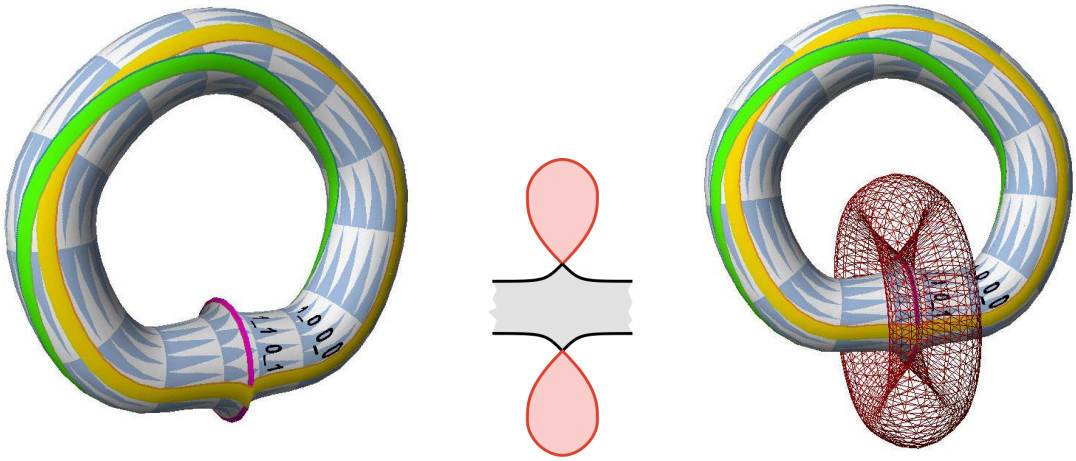

Figure 7: *Creating immersed tori with a "gluing" operation: (a) a torus with a cusp along a meridian; (b) "drop"-shaped cross section for the add-on part; (c) resulting representative for type* **O8**.

Moreover, any other toroidal structure in which the parameterization has been changed in some way must also belong to one of the four regular homotopy classes, and we should be able to find a sequence of smooth homotopy-preserving moves that convert any such "novel" torus into the appropriate generic representative. This applies to tori that wind multiple times around the big loop, or those that have their parameterization swapped through 90° (exchanging the roles of meridians and parallels), or even for a torus that has been turned inside-out. In the following I will describe a few generic moves, in addition to the F8SwXo- or CrF8Sw-moves, that preserve the regular homotopy class of the given surface.

5. Regular Homotopy Moves

Turning a Torus Inside-Out

On the web one can find several references to the process of *Torus Eversion*. In particular Cheritat presents an elegant and easy-to-understand video that shows this process [3] (Fig.8a). A closely related process is described in diagrammatic form by [2] (Fig.8b).

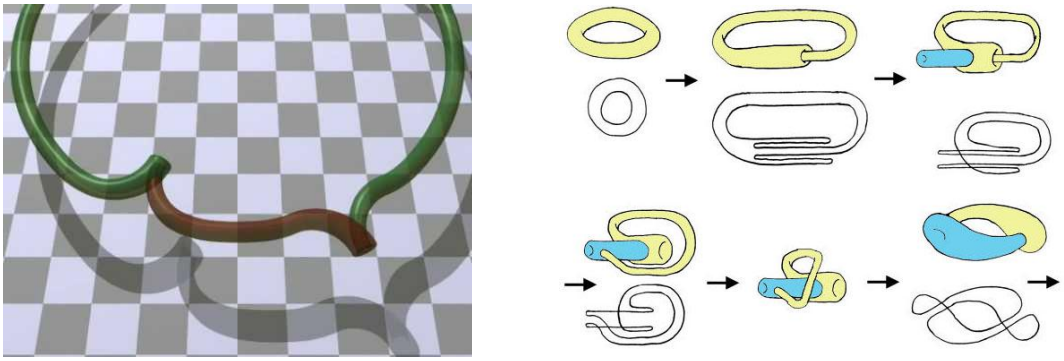

Figure 8: *Turning a torus inside out: (a) movie [3]; (b) schematic diagram [2].*

Figure 9 shows my own diagrammatic depiction of this process. During the whole process, the sweep curve remains planar, and I can thus depict the whole transformation by simply showing two opposite parallels (two equatorials) in orange and green, respectively, which are the intersection lines of the torus with the equatorial plane. Portions of the toroid, where surface parts that were originally facing inward have become exposed to the outside, are shown as dashed lines; this makes it obvious that the torus gets turned inside-out.

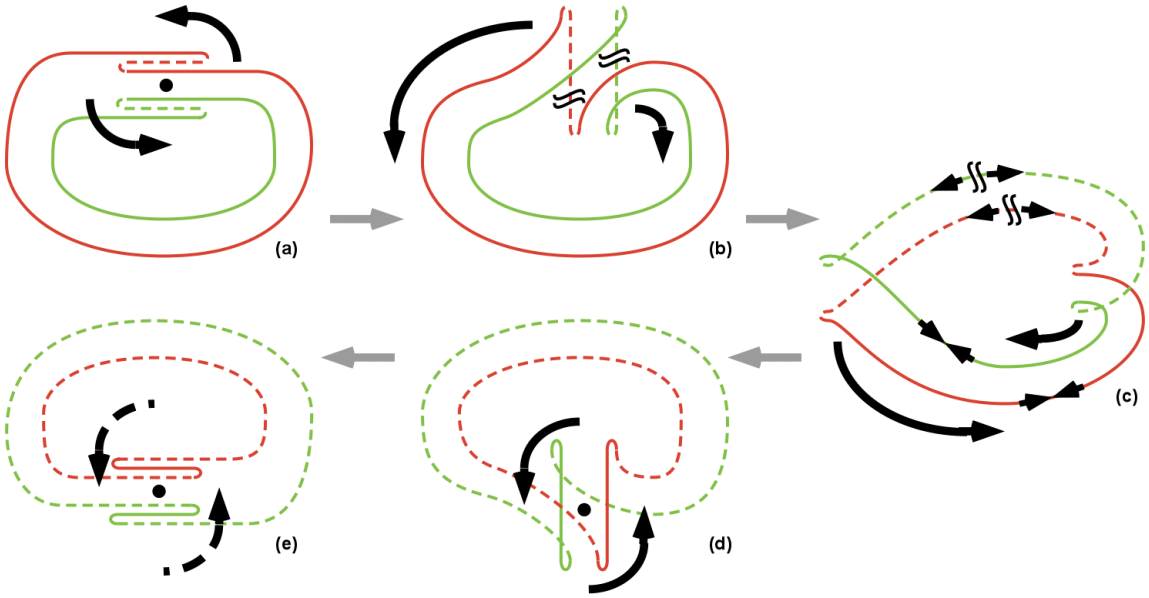

Figure 9: *Turning a torus inside out: (a)→(e) schematic view of two parallels (equatorials).*

The process starts by introducing a rotationally symmetrical fold around some meridian in the torus (Fig.9a). The everted tube segment is then turned through 90° (Fig.9b) and further turned and stretched, so that the two "Klein-bottle mouths" that delimit this segment can be moved apart (Fig.9c). They are moved in opposite directions around the toroidal loop. On the other side of the loop they are recombined into a short, straight tube segment (Fig.9d). This tube segment is then turned into alignment with the toroidal ring (Fig.9e) and unfolded in place.

All these moves are "planar" operations and thus they introduce no twisting of any kind. The 3-layer fold introduced in Figure 9a can also readily be generated for a tube with a Figure-8 cross-section. Moreover, the two Klein-bottle mouths have no problem passing through the (topologically irrelevant) cross-over intersection generated by a figure-8 sweep path. Thus this eversion process is directly applicable to tori of all four regular homotopy types.

Changing Parameterization and Profile

Another planar transformation that introduces no twist allows us to swap the parameterization and exchanging the roles of parallels into meridians (Fig.10). We introduce a triple fold into a torus of Type **O8** and maintain the resulting inverted segment as the core of a future "tubular" torus. By sliding the lobes of the figure-8 loop next to the inverted segment trough one another, we obtain just a simple loop connected to the inverted segment. When we let this loop contract, we realize that the new meridians formed have a figure-8 shape and thus are twisted (Fig.10d). The result is a Type **8O** torus with swapped parameterization.

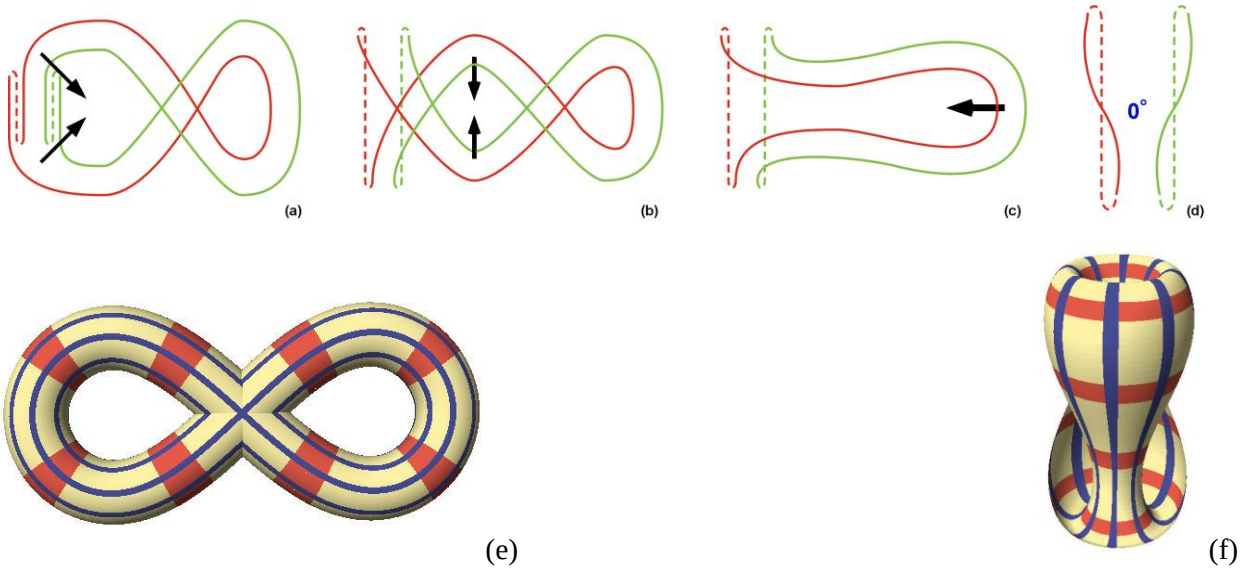

Figure 10: *Swapping the parameters is equivalent to switching between torus Type* **O8** *and Type* **8O***; (a → d) schematic transformation, (e, f) 3D models of the beginning and end states.*

If we try to do a similar operation on a torus of Type **OO** (Fig.11a), we find that we cannot collapse the loop without moving its sweep path out of the equatorial plane. The loop has to be un-tangled by going through the 3rd dimension (Fig.11b). This 180° flip introduces an M-twist of 360° into the contracting tube segment (Fig.11c). The previously untwisted parallels have now become untwisted diagonals in this Type **8O** torus with a 360° E-twist. We have achieved a swap of the parameterization combined with a profile change and the introduction of 360° E-twist.

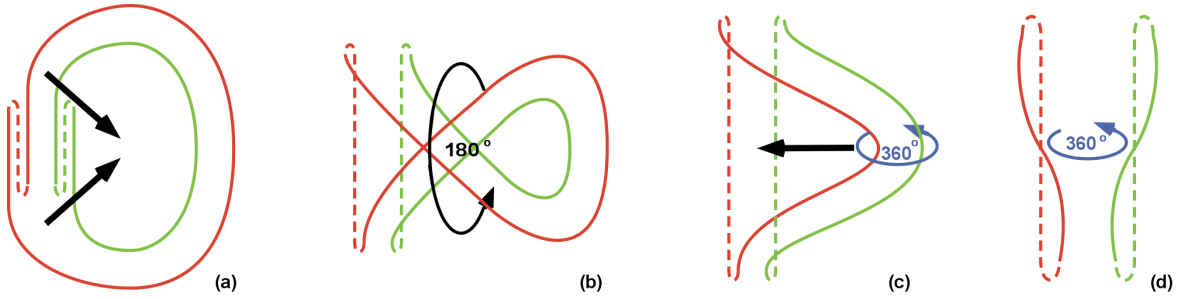

Figure 11: *Turning a torus of Type* **OO** *into Type* **8O** *with a twist and swapped parameterization.*

For completeness we show that this same transformation can also be visualized in a somewhat different way. We start with the same triple-fold, but then turn it by 90° (Fig.12a,b). Now, in order to collapse the downward dangling loop, we have to perform half of a *Dirac Belt Trick* move (Fig.13). This again is a move through 3D space that will add 360° of M-twist to this loop (Fig.12c), which then ends up as 360° of E-twist in the final torus (Fig.12d).

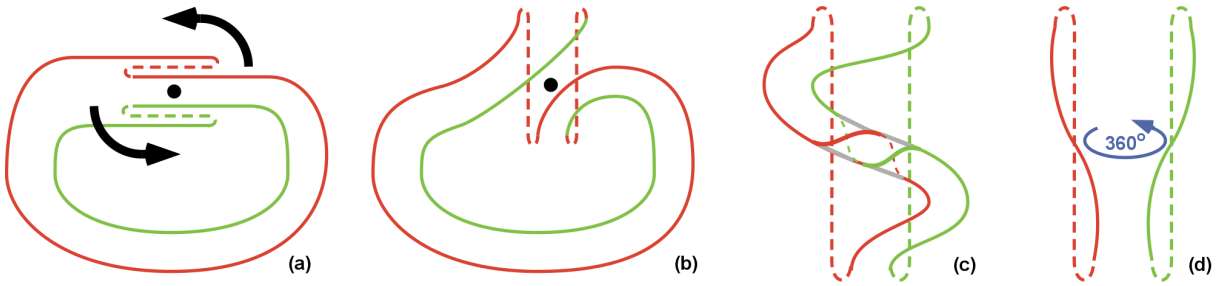

Figure 12: *A way to visualize the transformation shown in Figure 11, based on Dirac's Belt Trick [5].*

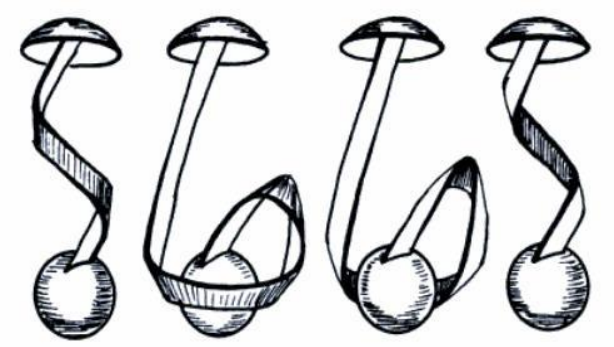

Figure 13: *Dirac Belt Trick illustrated by George Francis [5].*

Adding Dehn Twist

At this point it is worthwhile to point out that there is a simple operation to add any incremental E-twists of ±720°, which would be equivalent to a "cut-twist-reconnect" operation along an equatorial cut line. Figure 14 shows how one can grab the inner wall of a tubular torus, pull it sideways through the outer wall, and subject it to a complete F8SwXo-move (Fig.14b and 14c). This will introduce an M-twists of ±720° into this tubular loop, which then results in a ±720° E-twist in the final torus.

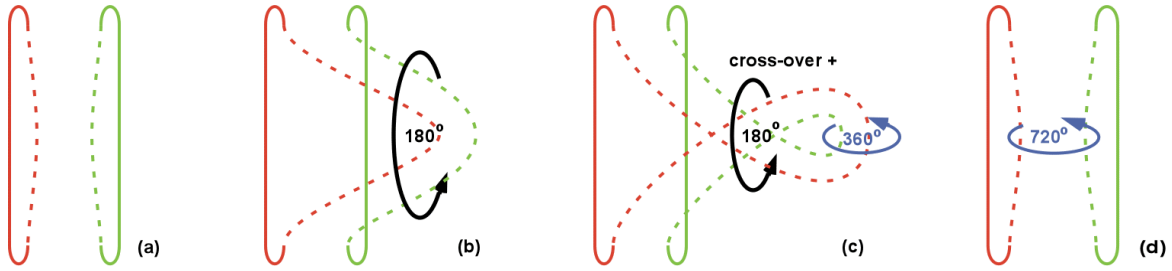

Figure 14: *Introducing an incremental E-twist of ±720° with two half-flips of a loop of the inner tube.*

Eliminating the Bulge in Figure 7c

With a move very similar to the one depicted in Figure 9, we can also turn the "novel" torus representative shown in Figure 7c into a piece of tubing with a built-in E-twist of 360° (Fig.15). Because the nature of the initial fold in this toroid (Fig.15a,b) is different from the one in Figure 9a, the transformed tubular torus ends up with a stretched "circular" cross section (Fig.15d), rather than one of figure-8 shape. But because this resulting "ordinary-looking" torus has a built-in E-twist of 360° and swapped parameterization, our question as to which class that surface belongs is still not fully answered. We first will have to study in a more general way how the homotopy class of a torus is changed through the introduction of some M-twist or E-twist of 360°.

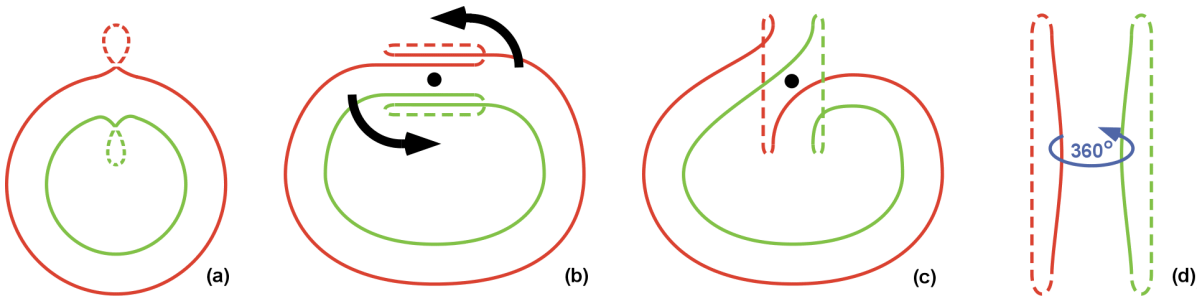

Figure 15: *Transforming Figure 7c into a tubular torus with 360° E-twist and swapped parameters.*

6. Torus Re-Parameterizations

So far we have looked at sequences of transformations that leave the surface in the same regular homotopy class. Now we turn the question around and explore how the homotopy type changes as we modify the surface parameterization in various ways. The operations that we can perform on the parameterization of a torus include:

Evert: Turning the surface of a torus inside out;

Twist: Adding E-twists or M-twists of ±360°;

Swap: Swapping the roles of the meridial and parallel parameter lines.

We have already seen (Fig.9) that the eversion process, which is equivalent to reversing (mirroring) the direction of exactly one of the two parameterization axes, keeps any of the four types of tori in the same regular homotopy class. Based on the discussions associated with Figures 4 and 5 we also know that the introduction of an M-twist of 360° switches a torus back and forth between Type **OO** and Type **O8**; and Figure 10 tells us that the swapping operation, i.e. a 90° rotation of the parameter grid, converts Type **O8** into Type **8O**, and vice versa.

For a convenient overview over the effects of the many different re-parametrizations possible, we introduce the map in Figure 16. It shows the four types of tori symbolically in the four gray circles, including a diagram of the geometry of a key representative as shown in Figure 1 and a characterization of the twistedness ("*u*" / "*t*") of three characteristic ribbons. All untwisted circular loops, like the meridians and parallels in Type **OO**, are characterized by u=1. But if we connect a paper strip into a figure-8 loop without any twisting, then we find, when we open the figure-8 path into a circular loop, that the ribbon now shows a 360° twist; such a ribbon is characterized by t=1. Since we can always add or subtract twist in increments of 720° with a F8SwXo-move, twist is counted modulo 2, and thus twist is always either 1 or 0.

An important insight is that *un-twistedness u*, the complement of twist t, defined as $u = (1–t) \bmod 2$, is more important than twist itself [16]. The value of u is directly linked to the turning of the *Darboux frame*, the local coordinate system that is used in differential geometry to describe the behavior of curves on surfaces. For the planar meridians and parallels the turning number modulo 2 sets the value of u. This makes u an additive quantity when we concatenate multiple ribbon loops [16]. Thus the doubly-looped meridians in Figure 2d have $u = 2 \pmod 2 = 0$; which implies $t = 1$; meaning they are twisted! But ribbons passing around a circular loop an odd number of times are untwisted. The u-values of two different characteristic ribbons allow us to unambiguously characterize each of the four regular homotopy classes of a torus by the four possible combinations of 1 and 0 for the u-values of two characteristic ribbons (e.g. meridians and parallels). With this knowledge we can calculated the u-values for arbitrary (m,p)-diagonal ribbons from the u-values of the meridians and parallels: $u_d = (m*u_m + p*u_p) \bmod 2$. With some simple matrix calculations we can then readily verify all the transformations depicted in Figure 16.

The double-headed arrows in Figure 16 indicate possible changes to the parameterization of the surface "texture" of the torus. The 2-by-2 matrix that accompanies the text label associated with each arrow specifies a coordinate transformation in the fundamental domain of the torus and thus characterizes how the transformation affects the roles of the meridians and parallels. An **eversion** matrix is an identity matrix in which the direction of one of the axes is reversed. The **swap** matrix has "1"s only on the minor diagonal, thus exchanging the roles of the two parameter axes. The matrices that represent the addition of **twist** are basically shear matrices. The amount of shear added is equal to the edge-length of the fundamental domain, which corresponds to an addition of 360° of Dehn twist to the torus surface. Dehn twists are only allowed in increments of ±360°, so that all previously closed lines close back onto themselves again after the addition of that twist.

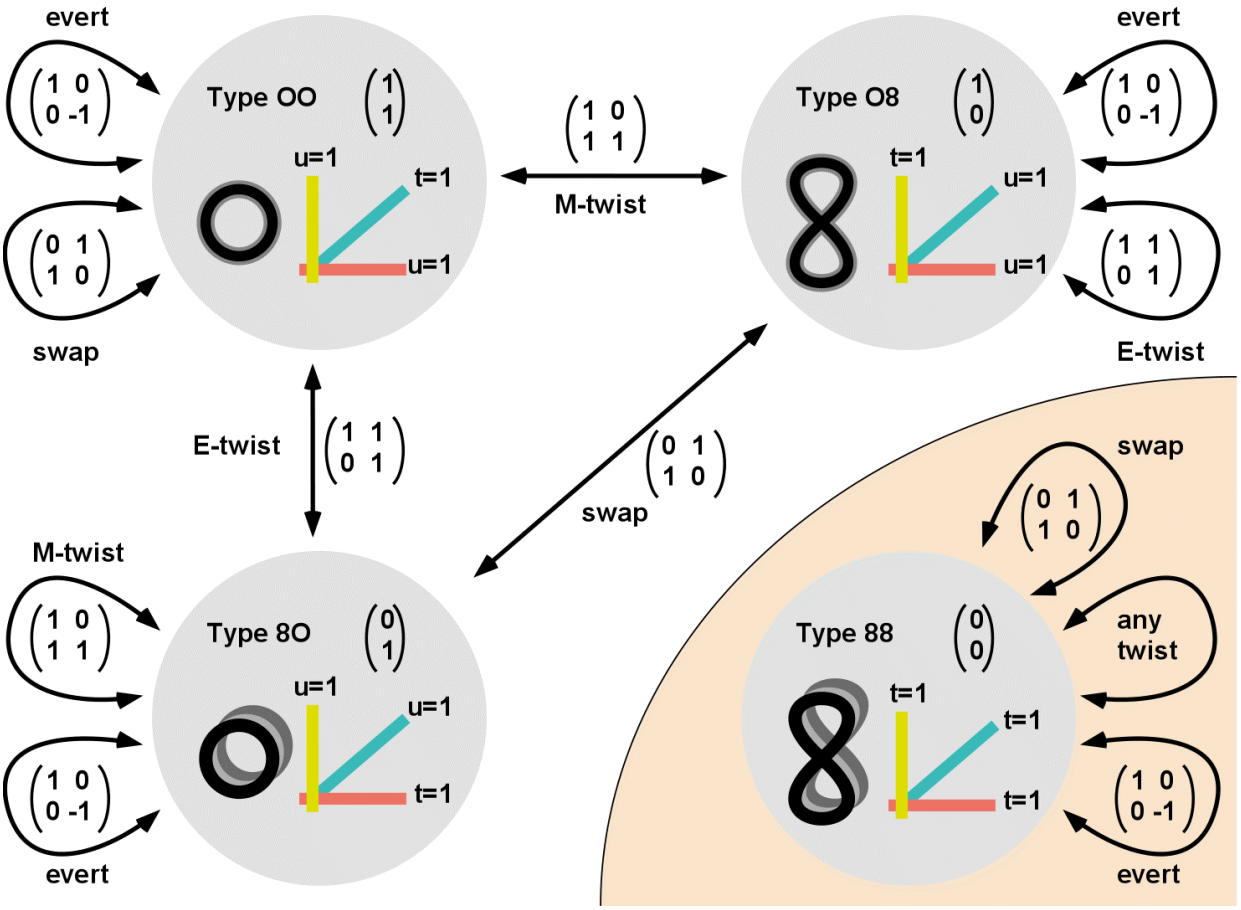

Figure 16: *Complete map of the effects of re-parameterizations on the different torus immersion classes.*

These matrices are transformations of the parameterization only. They should not be confused with the homotopy-preserving transformations discussed in Sections 3 to 5, which change the actual geometry of the torus. However, using these matrices, we can readily determine the resulting torus type in the form of its characteristic 2-component column vector; it is obtained by multiplying the 2-component column vector of the starting configuration on the left with the matrix of the parameter transformation in question:

$$\begin{pmatrix} a & b \\ c & d \end{pmatrix}\begin{pmatrix} m \\ p \end{pmatrix}=\begin{pmatrix} m' \\ p' \end{pmatrix}$$

We can double-check a few such operations and convince ourselves of the correctness of the outcome.

For instance: Does applying an M-twist to type **8O** really leave the type unchanged?

Answer: Adding 360° of M-twist does not change the geometry of the surface; it only shears the parameterization along one figure-8 meridian by shifting the domain on one side of such a meridial cut through the full figure-8 loop. The turning number along this loop is zero; thus any ribbon that ended on that cut (parallels and diagonals) and is being shifted around the whole loop does not gain or lose any twist. The meridial ribbons do not experience any changes either. Thus the type remains indeed the same.

Another way to summarize the results of various transformations is the following listing of the many ways in which tori belonging to the four different classes can be obtained:

Tori of Type OO:

- The standard untwisted torus – the chosen generic representative (Fig.1a);
- Everted type **OO** torus (Figs.9, 16-29);
- Type **OO** torus with swapped parameterization (Figs. 32-37);
- Everted and swapped type **OO** torus (Figs.32-36);
- Type OO torus with a even number of collars (Figs.23, 24);
- Any of the above with 720° of M-twist added (Figs.4, 5);
- Any of the above with 720° of E-twist added (Fig.14);
- Type **O8** torus with 360° M-twist (Figs.4, 5);
- Type **8O** torus with 360° E-twist and swapped parameters (Fig.11).

Tori of Type O8:

- A circle swept along a figure-8 path – the chosen generic representative (Fig.1b);
- Everted type **O8** torus (Fig.9);
- Type **8O** torus with swapped parameterization (Fig.10);
- Type **O8** torus with any (integer) E-twist (Fig.16);
- Type **OO** torus with an M-twist of 360° or **odd** multiples thereof (Figs.4, 5);
- A doubly-wound toroidal loop without twist (Fig.18);
- Type OO torus with an odd number of collars (Figs.23, 24).

Tori of Type 8O:

- A figure-8 profile swept along a circle – the chosen generic representative (Fig.1c);
- Everted type **8O** torus (Fig.9, 26);
- Type **O8** torus with swapped parameterization (Fig.10);
- Type **8O** torus with any (integer) M-twist (Fig.16);
- Type **OO** torus with an E-twist of 360° or **odd** multiples thereof (Fig.11);
- A doubly-rolled cylinder bent into a circular toroid (Fig.19).

Tori of Type 88:

- A figure-8 profile swept along a figure-8 path – the chosen generic representative (Fig.1d);
- Everted type **88** torus (Fig.9, 27);
- Type **88** torus with swapped parameterization (Fig.16);
- Type **88** torus with any (integer) E-twists or M-twists (Fig.16)
- A doubly-rolled cylinder forming a circular loop with 360° of M-twist (Fig.19).

Where possible, I have listed figures that illustrate corresponding homotopy-preserving transformations. Some of them will be discussed in later sections. Ideally, I would like to have an explicit, simple, and smooth transformation sequence for every arrow in Figure 16. Of special interest are the transformations that turn a torus inside out and those that swap its parameterization, and I will look at those more closely later in the report. But first I will discuss the classification of some rather unusual tori.

7. Analysis of Arbitrary Torus Structures

We will now give some examples of some wild and weird torus structures and show how they can be analyzed and assigned to the proper regular homotopy class. The simpler cases can be classified easily by inspection of the above table or Figure 16. But there are perfectly legal tori structures whose shapes go way beyond some simple twisting and/or re-parameterization. The different ways of forming tubes (Fig.2) and then closing them into toroidal loops (Figs.3-7) can be combined in many intricate ways!

Multi-Loop Tori

A tube of any given cross-section can be coiled through multiple loops before the ends are joined to form a topological torus. An intriguing example is shown in Figure 17a. Here a tube with a roughly triangular cross section is coiled into a self-intersecting double loop and closed with an overall twist of 360°. To better understand this structure and its cross section, it is also shown in a segmented version (Fig.17b).

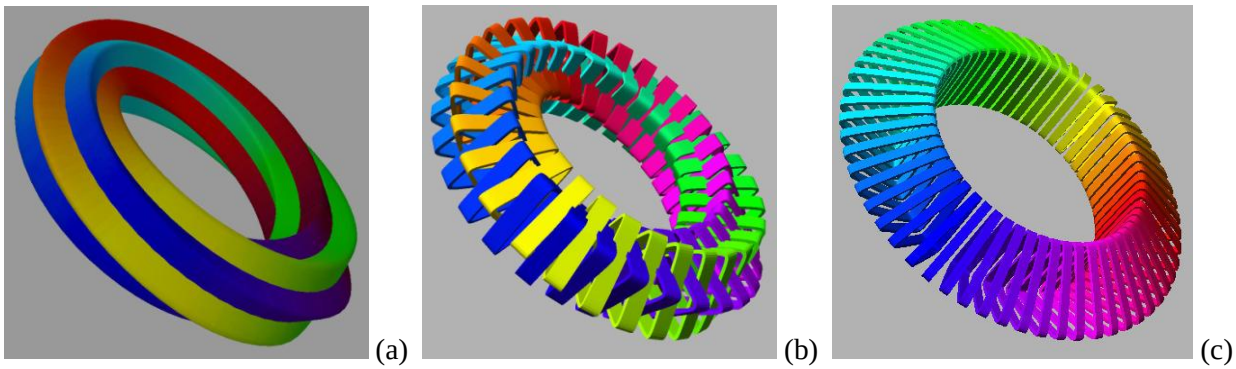

Figure 17: *(a) Doubly-looped torus with triangular cross section and 360° twist; (b) the same torus segmented for easy visualization; (c) the same structure after unwinding it into a circular sweep.*

Such a doubly-looped structure can be unfolded smoothly into a figure-8 shape (Fig.18). The azimuth of the texture in the moving branch-loop gradually changes through 180° (The yellow parallel on the right hand loop shifts gradually from the inside of the loop to its outside in Figures 18b and 18c.), but there is no new twist introduced into the tube anywhere.

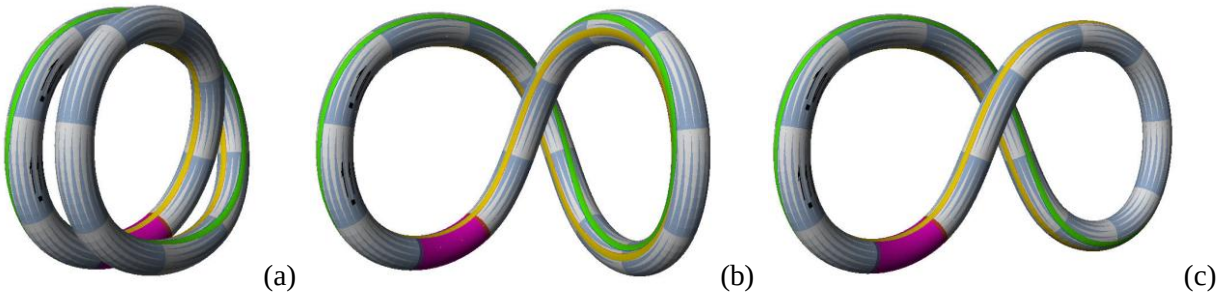

Figure 18: *(a) Unwinding a double loop into a figure-8 path without changing twist: (a) starting state, (b) halfway point, (c) final state.*

Of course, if we now untwist the figure-8 path into a simple circle, the tube will experience an incremental twist of 360°. In the torus shown in Figure 17, this incremental twist-change cancels out the original twist, so that the final result is just a twist-free torus of type **OO** (Fig.17c).

Multi-Rolled Tubes

Figure 19a shows another intriguing torus, with a profile resembling a curtate hypocycloid. In Figure 19b the loop has been cut open and its twist removed, so that one can better understand its cross section. Figures 20a-20c show that this cross section, exhibiting a turning number of 2, can be smoothly transformed into a double circle. So the basic structure of this tube is just the doubly-rolled cylinder (Fig.20d), which we have encountered already in Figure 2d. Now we want to turn this torus (Fig.19a) into one of the four generic representatives.

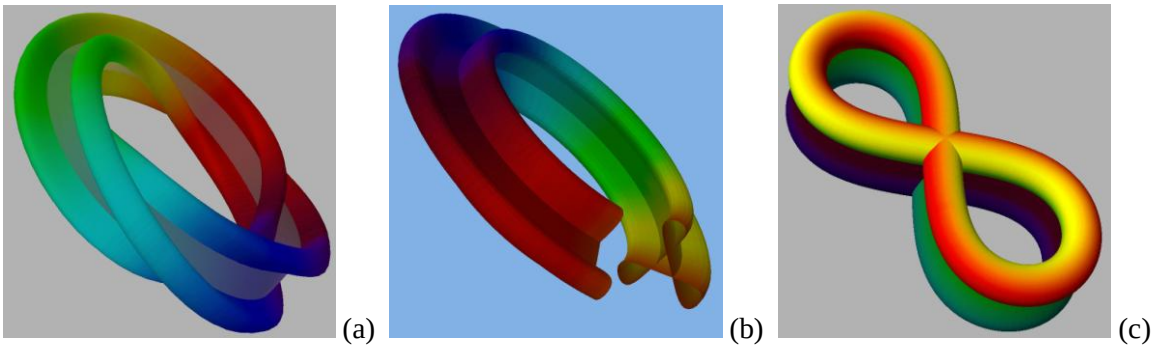

Figure 19: *(a) Unwinding a doubly-rolled torus into a double loop with a figure-8 profile: (a) starting state, (b) cut open and untwisted, (c) after parameter swap.*

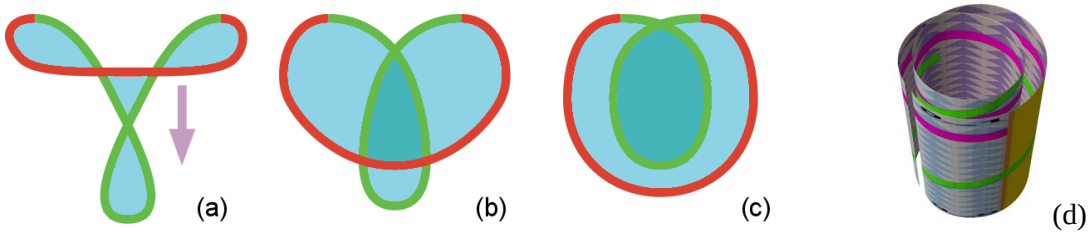

Figure 20: *(a → c) Transforming a curate hypocyclic profile into a double roll, (d) the resulting tube.*

We use a transformation that combines a parameter swap with a profile change (Figs.10, 11). But this time we start with 360° of twist in the original structure, and we need to show double walls everywhere because of the doubly rolled tube (Fig.21). In the swap process, the double roll turns into a double loop. The 180° flip of the crossed lobe (Fig.21b) removes the original twist of 360°, and the profile changes to a figure-8 shape (Fig.21d). This double loop can now be unfolded (Fig.18) without adding twist. Thus we end up with the generic representative of type **88**.

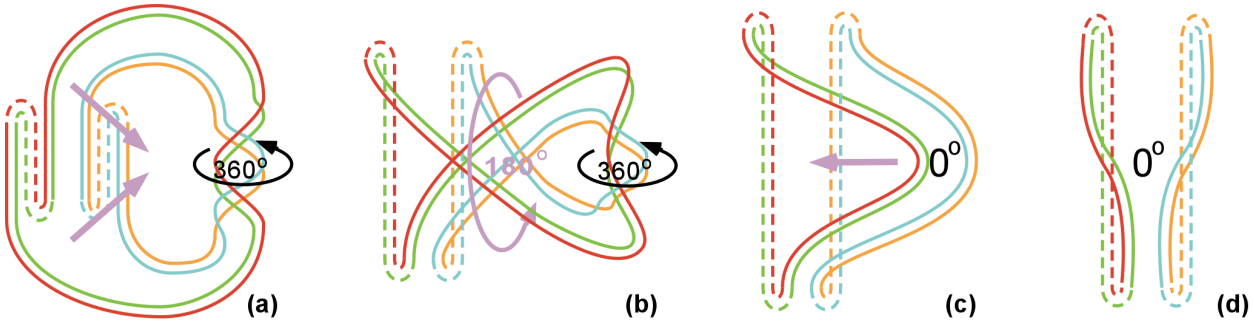

Figure 21: *(a → d) Transforming a doubly-rolled torus into a torus with a double loop.*

Tori with Collars

In Figure 7 we have encountered a torus with a collar. I concluded that this torus must be of type **O8**, but I have not yet shown a process by which this collar can be removed. Figure 22a shows another torus with a collar; and, of course, tori can have more than just one collar (Fig.22b). Moreover, collars can lie on the inside of the toroidal tube (Fig.22c) just as well as on the outside.

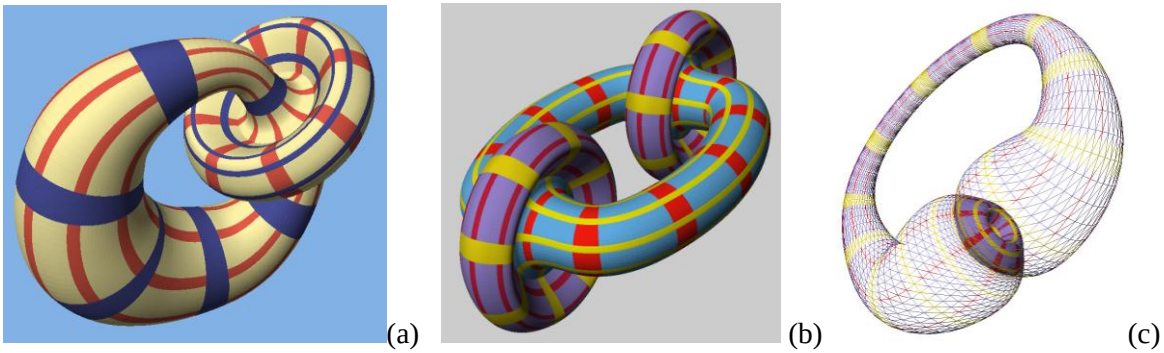

(a) (b) (c)

Figure 22: *Tori with collars: (a) a single collar on the outside, (b) two collars, (c) inside collar.*

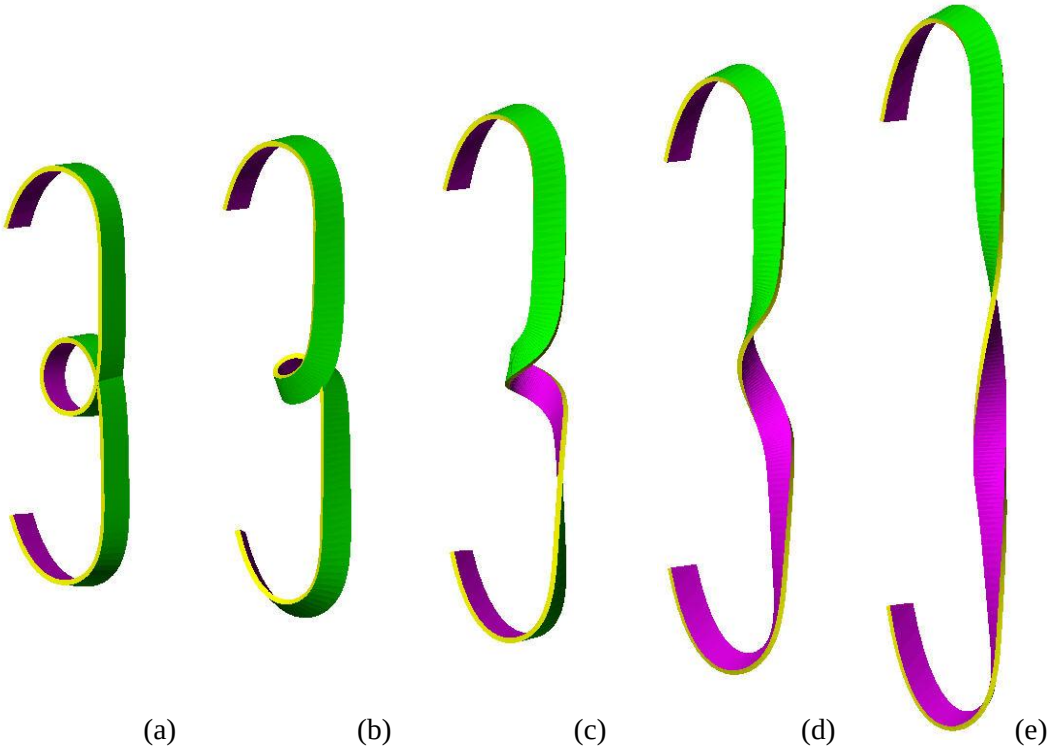

(a) (b) (c) (d) (e)

Figure 23: *(a → e) Unwinding a collar loop into 360° of twist using the Dirac Belt Trick [5].*

An operation based on the Dirac Belt Trick [5] allows us to remove such a collar and convert it into 360° of M-twist in the torus tube. The principle is illustrated in Figure 23. As the belt is stretched, the loop in its middle turns into a full twist of the belt. This fact can used for the removal of a collar in the same way that it was used in the movie *Outside-In* [8] to evert a sphere. The surface near the collar is partitioned into sufficiently many corrugated rib-segments (8 were used in [8]), which are flexibly connected to one other through equally many "bellows." These bellows provide the necessary flexibility so that the surface can perform this un-winding manoeuvre of the collar loop without experiencing any kinks.

Figure 24 shows a collection of bands representing neighboring corrugations and illustrates how the collar can be un-done while jointly swinging one end of all the belts 360°around the torus tube. At the end of this process, the ribbons form full 360° helices, but lie nicely embedded in the cylinder surface. If there is more than one collar in a torus, each one can be turned into ±360° of twist; so pairs of collars can actually annihilate one another without creating any net twist.

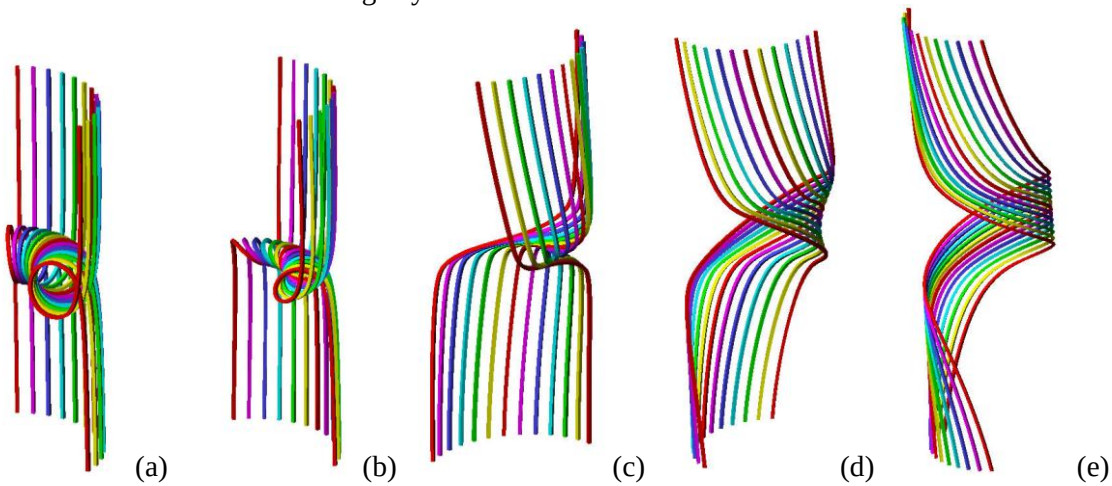

Figure 24: *: (a → e) Unwinding an internal collar with into 360° of M-twist.*

Tori with Internal Knots

As a final example of tori classification we look at the sculpture in Figure 25. Here an ellipsoidal body is penetrated by an internal tunnel, which itself is knotted into a figure-8 knot (Fig.25a). The knot can be readily pulled apart into a straight tunnel, since torus branches can pass through one another. But the question arises, how much twist is produced in this process, and how much twist there was to begin with. To answer these questions, the most direct approach simply analyzes the twistiness of the meridial and parallel grid lines. Looking at Figure 25b, it is clear that the yellow parallels are untwisted. The long, knotted gridlines that run parallel to the sweep path of this tube are more difficult to analyze. But it is possible to take a narrow paper-strip and bend it so that it follows the contortions of the surface along the path of one of these grid lines. Then one can tape the two ends of the strip together, stretch out the loop, and readily examine how much twist there is. In this example, there is no twist. Thus, since both complementary grid line ribbons are without twist, we have just an ordinary torus of type **OO**.

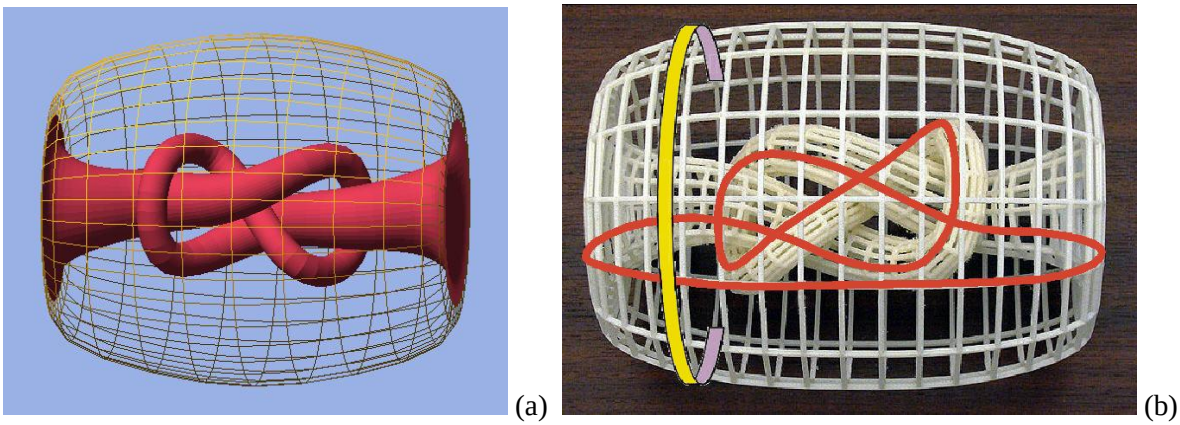

Figure 25: *Torus with an internal figure-8 knot. (a) The basic structure of the knotted tunnel; (b) analysis of the twistedness of the parallel (yellow) and meridial (red) parameter ribbons.*

8. More on Torus Eversions

Having accumulated a sizeable collection of torus transformations, we can now revisit some of the previous transformations and explore alternatives. Just as there is more than one way to evert a sphere [8] [9] [10] [11] [14]; there are also several ways to do this for the torus. Quite surprisingly, several of these methods are quite easy to visualize. We have already seen one method, depicted in Figures 8 and 9. The goal now is to find the "simplest" and most "elegant" process. Below are some alternatives, some of which work only on a subset of the four tori types.

Easy Eversions for Tori with a Figure-8 Profile

For tori of types **8O** and **88** there is a very simple process to turn the surface inside-out: We can just shift the parameterization in the meridial direction through half of the figure-8 profile (Figs.26 and 27). This brings portions of the surface that were facing outwards to locations where they are now facing inwards, and vice versa. For a torus of type **8O** to which the texture shown in Figure 27a has been applied, the process starts with Figures 26a, 26b. In (a) both sides of the surface are rendered, but back-facing elements (here the green ones) are rendered darker, and the text appears mirrored in those areas. In (b) back-face suppression has been turned on, so we can see how the front-side of the surface wraps from the outside to the inside of the figure-8 profile. In (c) we have started to shift the texture in the meridial direction (about 6%), with the yellow parts ("BULGE 1") moving downward on the outer side of the upper lobe in the figure-8 profile; they now start to appear on the inner part of the lower lobe. In (d) this shifting process has progressed to about 12%, and the green parts ("BULGE 2") start to appear at the top of the ring. Figure 26e shows a 33% shift of the texture, and in (f) we have reached the desired 50% shift which effectively turns the torus surface inside out. In (g) back-face suppression has been turned on, so we can see the inside portions of the lower lobe. If we now flip this modified torus through 180° in 3D space (Fig. 26h, 26i), we can readily see that the text in the texture has been reversed in the equatorial direction. Figure 26h shows only the front-facing elements, while (i) shows both sides of the surface. In this eversion process, the lighter parts of the surface have become darker, indicating that we now look at the backside of these portions, and correspondingly, the formerly darker surface parts (seen originally from the backside) now appear brighter, since we see them from their front sides.

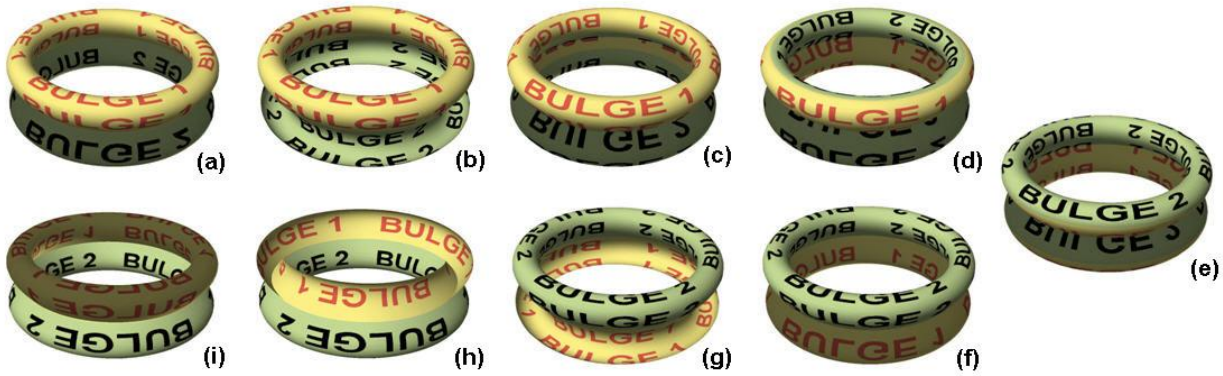

Figure 26: *(a → i) Eversion of a torus of type* **8O** *by shifting the surface 50% in the meridial direction.*

The same eversion process can also be applied to tori of type **88**, either in their figure-8 path form (Fig.1d) or in their twisted form (Fig.6b or 6d). Figures 27b and 27c show the un-shifted and the 50% shifted texture on the torus, respectively. Figures 27d is a view of (c) flipped through 180° in 3D space, so that it can be compared more easily with Figure 27b. Again, the text has been reversed from left to right, and front surfaces have become back surfaces, and vice versa.

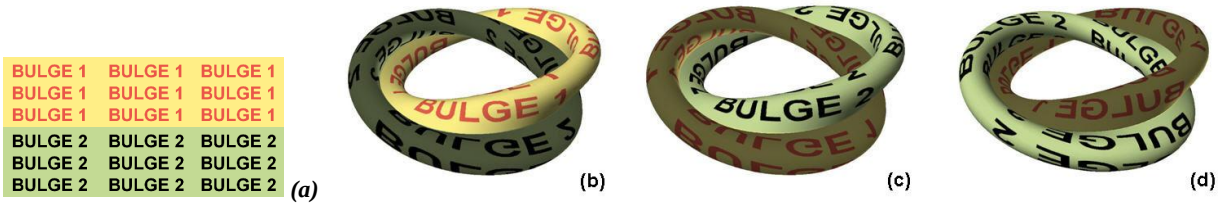

Figure 27: *(a) Texture used in Figures 26 and 27; (b → d) Everting a torus of type* **88** *by shifting its surface 50% in the meridial direction.*

Reuse of Figures 11a-d

Since it is so easy to evert tori with a figure-8 profile, we can transform tori with a circular cross section first into a shape with a figure-8 profile by using the processes shown in Figures 10 and 11, perform the torus eversion there, and then undo the initial transform. This is illustrated in Figure 28 for a torus of type **OO**. Once the original torus has been transformed into a tube with figure-8-shaped walls (Fig.28d), we can perform the eversion easily by either doing the parameter shift described above, or by simply flipping the figure-8 profile through 180° (Fig.28d, 28e). Then we reverse the transformation back to the original shape, but now with the surface turned inside out. This process is illustrated in Figure 28 where the walls have been drawn with double lines of two different colors to make the surface eversion more apparent.

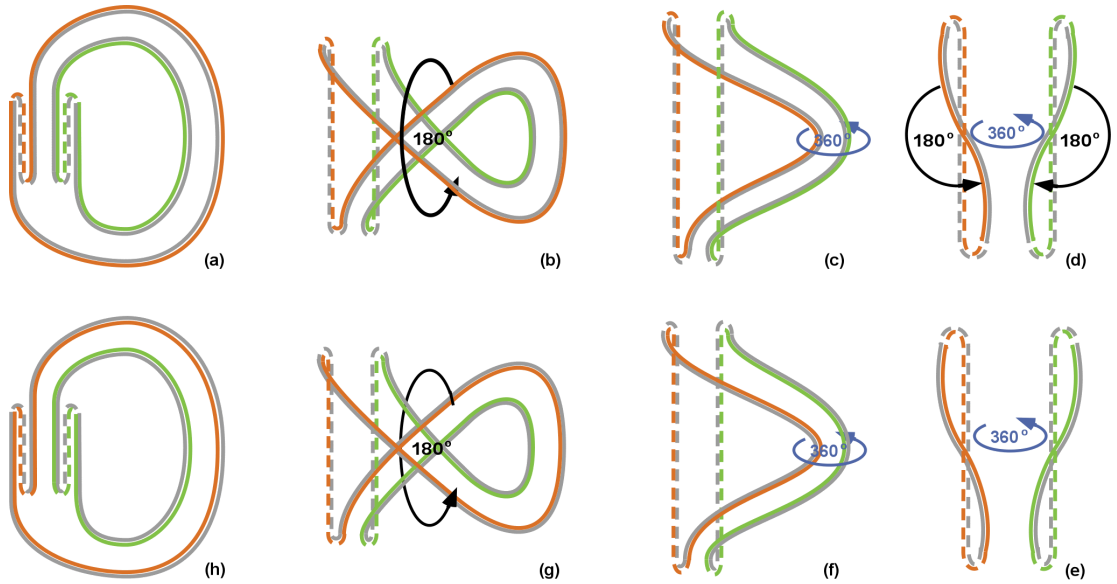

Figure 28: *(a → h) Turning a torus inside out by transforming it through the type* **8O** *half-way point.*

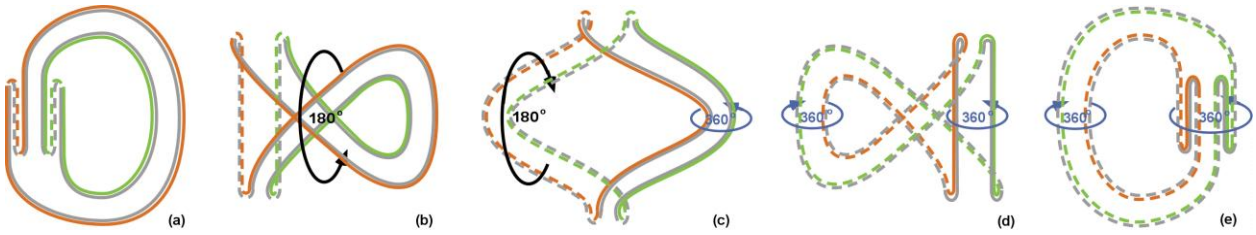

Figure 29: *(a → e) Taking a short-cut in the above process of turning a torus inside out.*

It should be pointed out that rather than flipping the wall of the tubular torus through 180° (Fig.28d, 28e), we can also bulge out the dashed wall section in Figure 28d and then retrace our steps towards the left, but now flipping **the dashed loop** through 180°, with the same end result. This is illustrated in abbreviated form in Figure 29. In the step from (b) to (c) we flip the solid loop through 180° while simultaneously bulging out the dashed segment towards the left. In the step from (c) to (d) we then flip the dashed loop through 180° while shrinking the solid segment into a straight tube. The directions of the two flips can be chosen so that the resulting meridial twists in the toroidal loop cancel out (Fig.29e).

Looking at this sequence of transformation steps, we can see that it is in principle the same as the process described in Figure 9. Rather than letting the two Klein-bottle mouths travel around the toroidal loop, we now keep them more or less stationary, pointing in opposite directions, and let the connecting tube segments carry out the necessary deformations and flips.

Minimum-Energy Processes

Among many possible ways to evert a sphere, the "Optiverse" process [14] has the fewest topological events and is energetically most efficient. This specific move sequence was found by first picking a suitable topological halfway point and smoothing its geometry to minimize its total surface bending energy. A slight asymmetrical disturbance is then introduced, and the surface evolves through ever lower energy states until it ends up as a sphere. We would like to find a similarly optimal process for the eversion of a torus. Towards this goal, we look for possible half-way points of the eversion process.

Figure 9c, as well as Figures 28d and 29c are all possible candidates. It should be noted that Figure 9c can readily be converted into Figure 29c by turning the inward-pointing Klein-bottle mouth outwards. In doing this, we will introduce 180° of M-twist (with opposite handedness) into each of the two halves of the toroidal loop. But by turning one of the two Klein-bottle mouths around its rotational symmetry axis, we can readily shift some of that twist from one branch to the other; thus we can render one branch completely twist-free and have the other one twisted by 360° as in Figure 29c.

Now let's take the half-way point in Figure 29c, simplify it, minimize its energy, and then examine whether it may serve as a way to generate a good torus eversion process. Figure 30a shows a surface corresponding to the geometry in Figure 29c after a few generations of surface optimization in Brakke's Surface Evolver [1]. This is a process that requires careful supervision by the user. Some problems start to show in Figure 30a: Some sharp dihedral angles have formed between some of the facets, and in this state the optimization process may do weird things: e.g. some lips and sharp creases may form that render subsequent optimization steps meaningless.

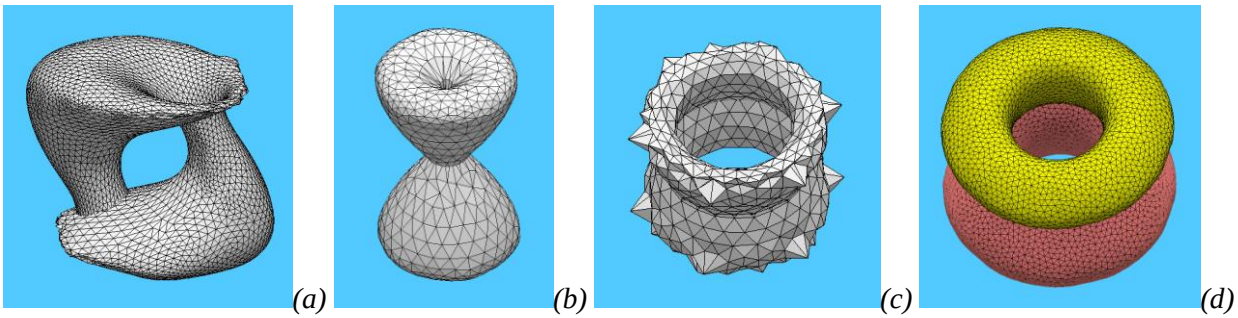

Figure 30: *Brakke's Surface Evolver applied to a surface corresponding to Figure 29c: Problems arise: (a) crease formation, (b) tunnel pinch-off, (c) spike formation; (d) finally a successful evolution.*

Since surface domains can readily move through one another (costs are derived solely based on area and curvature of the surface), this shape eventually evolves into a rotationally symmetrical configuration – if we can circumvent the convergence problems. This is possible by carefully interspersing *vertex averaging*

and *elimination of short edges* in between the regular surface optimization steps. But even a completely symmetrical starting geometry can have some problems. If the structure is too long and too slender, then the central tunnels will pinch off (Fig.30b). A shorter and wider starting geometry avoids that problem; but inappropriate step sizes may still lead to other problems such as serrated surfaces and protruding spikes (Fig.30c). However, with enough handholding of the *Surface Evolver* process, I eventually got to a plausible final smooth state with a very low energy value (Fig.30d).

Now the question arises, whether this shape can be used as an appropriate energy saddle point from where we can find down-hill paths to the two complementary eversion states of the ordinary torus. If we just consider the total bending energy of the surface, then the shape in Figure 30d has no reason to move in any new direction. However, unlike the case for the sphere eversion, we are now dealing with parameterized surfaces, and the shape of the parameter grid-lines is very important. The shape that we are currently considering has a total M-twist of 360° built into it, and this twist must exert enough of a penalty so that the optimization process wants to move out of this state.

Figure 31 shows a more informative rendering of the shape under discussion; now we show the actual twisted parameter lines. Figure 31a shows the state directly derived from Figure 29c, while Figure 31b depicts the state that would result if we are trying to simply minimize surface bending energy. But this optimization step is really counter-productive. It drives the surface into a state with too much symmetry, and we will have to break that symmetry to get back to a torus of type **OO**. Figure 31a is a much better starting point for this process. It already forms a roughly toroidal loop. We could push it in the direction where the green branch dominates and the two Klein-bottle mouths combine and wipe out the red branch between them to form a smooth torus. To do this, we would have to transfer the twist from the red branch to the green branch. Then, as shown in Figure 29, the dominant green branch will undergo a loop-flip through 3D space and thereby get rid of its 360° of M-twist, while the two Klein-bottle-mouths join to form a triple-fold than can be smoothly eliminated. Alternatively, we could let the red branch dominate when forming the final torus shape; we would then end up with the everted torus shape.

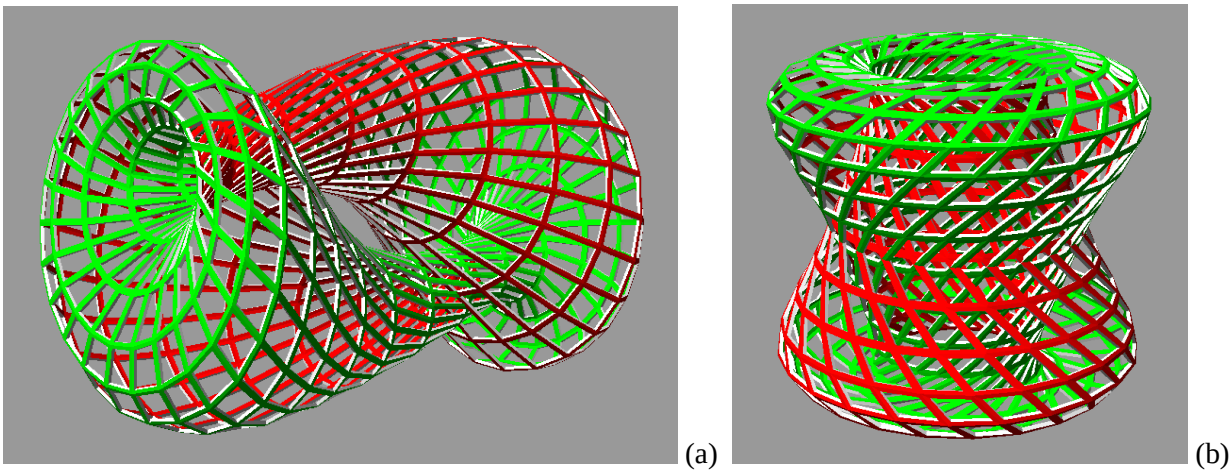
(a) (b)

Figure 31: *Symmetrical half-way points for a possible torus eversion process: (a) corresponding to Figure 29c, (b) corresponding to Figure 11d.*

How all of these events can be made to happen simultaneously in a smooth, energy-minimizing process is beyond my unassisted visualization capabilities. Future work will consist in creating an optimization system that can assign an appropriate penalty to skewed, non-orthogonal grid lines, which will create the forces that want to unwind any twist present so as to always end up in one of the four generic, un-twisted representatives of the four homotopy classes (Fig. 1). A detailed investigation needs to be carried out how to construct a suitable spring-mass model for a parameterized surface that explicitly represents the parameter lines (e.g., as in Figure 31), and which also has a suitably high penalty cost for twisted

(skewed) parameterizations. Such a penalty term may be derived from any non-orthogonal crossing of the parameter lines measured in a projection onto the tangent plane at every vertex.

A simple energy model for twisted tubes has recently been developed in joint work with Avik Das and Victor Huang. This model is capable of unwinding twisted toriodal loops into their untwisted base state with either a circular or a figure-8 sweep path. But it cannot yet handle the more complex cases of Klein-bottle mouths and more general free-form surface shapes.

At this point, I am reasonably confident that the optimal eversion process will have a half-way point that is some combination of the shapes depicted in Figures 9c and 31a. Thus the main task of an optimization system, with an appropriate energy functional that can account for twist, will be to figure out what shape of the half-way point will yield the lowest-energy saddle point for the whole torus eversion process.

9. Parameter Swap

The toughest challenge seems to be to find an elegant transformation that swaps the parameterization of the ordinary torus of type **OO**. I have not yet found a satisfactory, low-energy solution. Perhaps this is related to the fact that it is not intuitively obvious that one can indeed turn by 90° the parameterization of an ordinary torus so that meridians become parallels, and vice versa, via a continuous smooth homotopy-preserving operation.

Looking for a Plausible Half-Way Point

Again, we may start by looking for a nice, symmetrical half-way point between the two desired end-states, i.e., a torus immersion that is equidistant (in a transformational sense) from two tori of type **OO**, but with swapped parameterization. One possibility to construct a plausible halfway point starts with two interlinked tori with complementary (swapped) parameterization. The two tori are made to touch in one point and are lined up in such a way that near the contact point their parametrizations (i.e., their yellow and magenta ribbons) coincide (Fig. 32a). Now we consider the saddle surface created near the contact point (Fig.32b). It can be seen as either two intertwined handles or as two tunnels touching each other. This type of *Handle-Tunnel* combination can also be constructed directly by taking the rectangular domain of the torus, bending it into a saddle surface, and gluing the middle portions of the horizontal and vertical edge pairs together (Fig.32b).

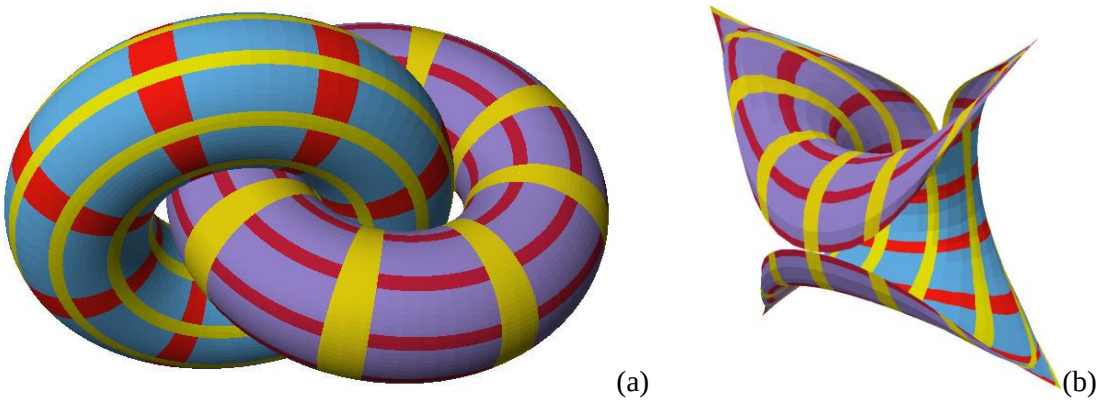

Figure 32: *(a) Two interlinked tori. (b) Saddle surface formed at the contact point.*

Now, if we choose to close the surface in Figure 32b by completing the torus colored blue on the outside, the magenta ribbons become meridians and the yellow ones turn into parallels. Alternatively, if we chose to complete the purple torus, the red ribbons become the parallels, and the yellow ribbons turn into meridians – thus yielding a torus with swapped parameterization.

In Figure 33 we look at this same situation from an immersed point of view. To form a complete torus, the square boundary of the depicted geometry has to be closed with an additional surface patch. We can do this in two different ways: We can close it with a surface that passes around the viewer and thus puts the viewer *inside* this structure. In this case the sweep path of the torus would be the horizontal loop shown in white, and the corresponding parallels would also be horizontal. Alternatively, we can close the torus domain away from the viewer, behind the image plane; this would yield an *outside* view of this (deformed) torus. Now the sweep path would be a vertical circle looping away from the viewer; and horizontal cuts through this structure would produce meridians. Thus going from one type of closure to the other, i.e. flipping the closing membrane from behind the viewer to behind the image plane, swaps the parameterization and also turns the torus inside out.

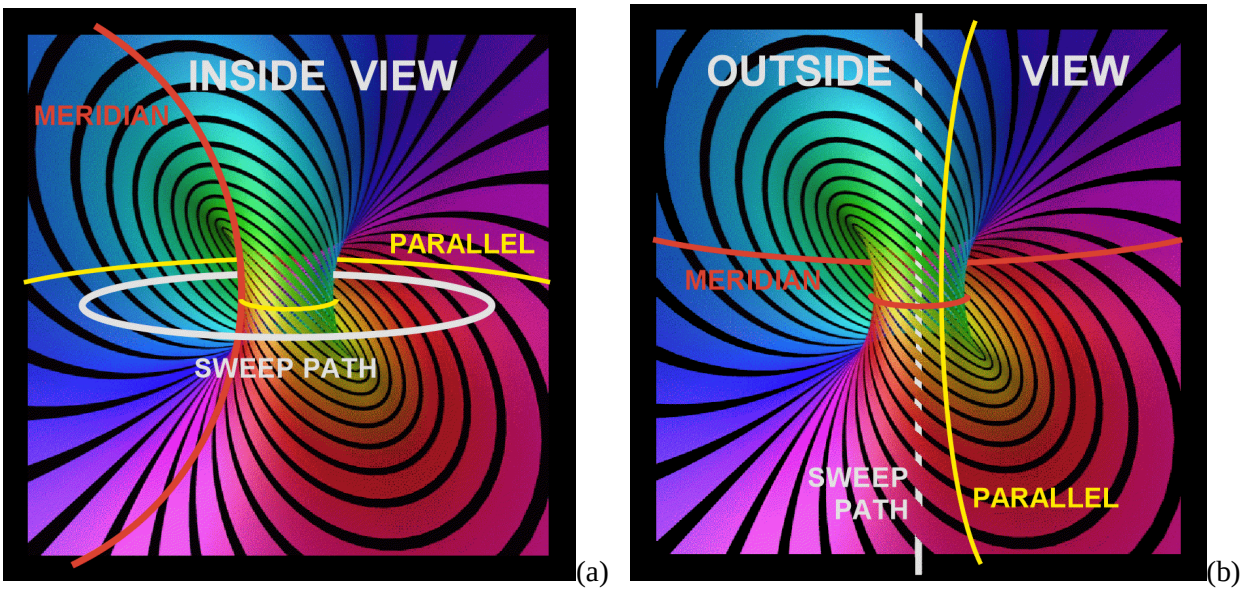

(a) (b)

Figure 33: *Handle-Tunnel shape with two alternative, conceptual "closures:" (a) with a surface piece (membrane) passing behind the viewer, (b) with a membrane passing behind the picture.*

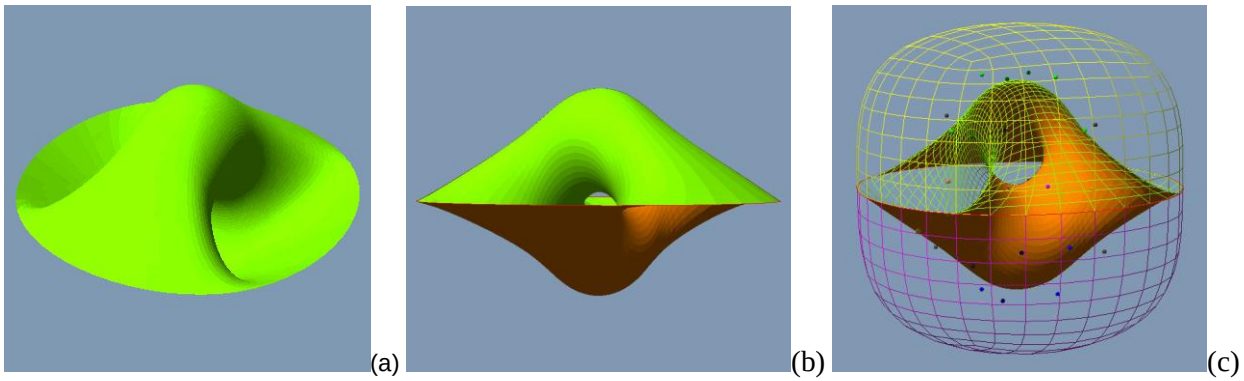
(a) (b) (c)

Figure 34: *(a) Handle-Tunnel shape with circular perimeter; (b) side-view of Handle-Tunnel shape embedded in a disk; (c) conceptual model for parameter-swap with two alternative "closures".*

The formation of the saddle surface shown in Figure 32b is topologically identical to a torus with a hole in its surface (the location where the four corners of the rectangular domain are supposed to meet). We now smooth out the rim of this piece of surface that contains the *Handle-Tunnel* geometry into a planar

circle. Figures 34a and 34b illustrate the resulting shape; the surface patch has been colored green on top and brown on its backside. To form a torus, this surface has to be closed with a membrane with the topology of a disk glued to its perimeter. Figure 34c shows two ways of doing this. In this figure only the brown backside of the surface has been rendered solid, while the front side is shown as a light green wire-mesh. Also shown in wire-mesh are two hemispherical membranes. If we use the lower, *bowl*-shaped closure, shown as a magenta wire-frame, we obtain one state of the torus; if instead we use the yellow, *dome*-shaped closure, we obtain the other state, which is an everted torus with swapped parameterization.

We can get rid of the unwanted surface eversion with the process depicted in Figure 9, and thus we could obtain the desired pure parameter swap – if we could legally switch from *bowl* closure to *dome* closure. But this is not so straightforward: Simply pushing the hemispherical membrane through the equatorial plane would produce some pinch-off points. And even the half-way point itself, where the membrane coincides with the equatorial plane, is not legal: It has four pinch-off points in the shape of Whitney umbrellas [15] at the corners of the square patch, where the membrane rim changes from curling upward to curling downward. This is illustrated in Figure 35c. As the membrane is pushed downward (Fig.35b) or upward (Fig.35d) from its mid-position, the Whitney umbrellas merge pair-wise and annihilate one another. The two end-states are thus clean and legal immersions. Unfortunately we cannot pass through an illegal half-way point with this simple conceptual process.

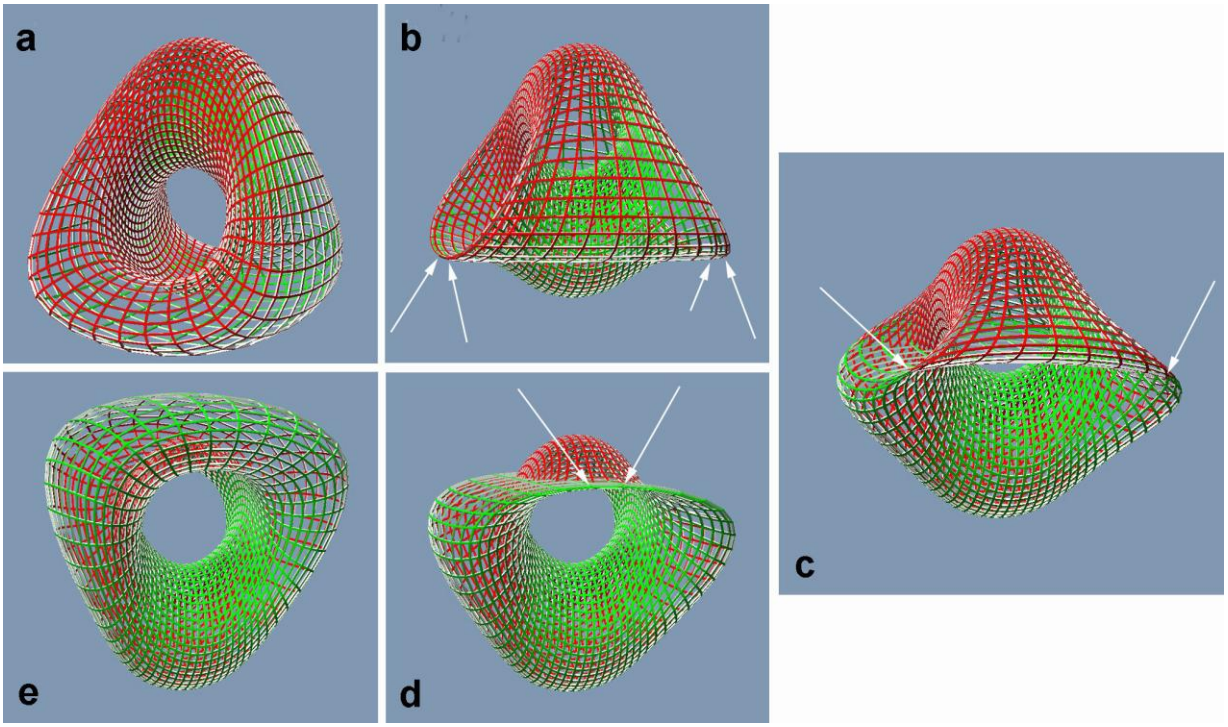

Figure 35: *Moving the closing membrane bottom to top through the Handle-Tunnel configuration.*

Using a Sphere-Eversion Process

Thus we need a more elaborate process to move the closing membrane from one side of the *Handle-Tunnel* configuration to the other. If, for the moment we overlook the detailed geometry of the two intertwined tunnels and just consider its circular equatorial perimeter and span it by a simple disk, then this disk together with the magenta *bowl* surface will form a topological sphere, and together with the yellow *dome* surface it forms an everted version of this sphere. Thus we can rely on a classical sphere eversion process to accomplish the needed switch from *bowl*-closure to *dome*-closure.

For a particularly nice visualization, we stitch the disk containing the *Handle-Tunnel* geometry into a small circular hole at the north pole of an ordinary sphere (Fig.36b) and then apply the "Outside-In" eversion process [8] (Fig.36a). In this process the polar region is simply shifted to the other pole along the globe's axis. At the same time, the closing surface moves from lying below it to lying above it and thus accomplishes the desired parameter swap combined with a surface eversion. Together with a simple, straight torus eversion (Fig.9) we can obtain a net parameter swap in a torus of type **OO**.

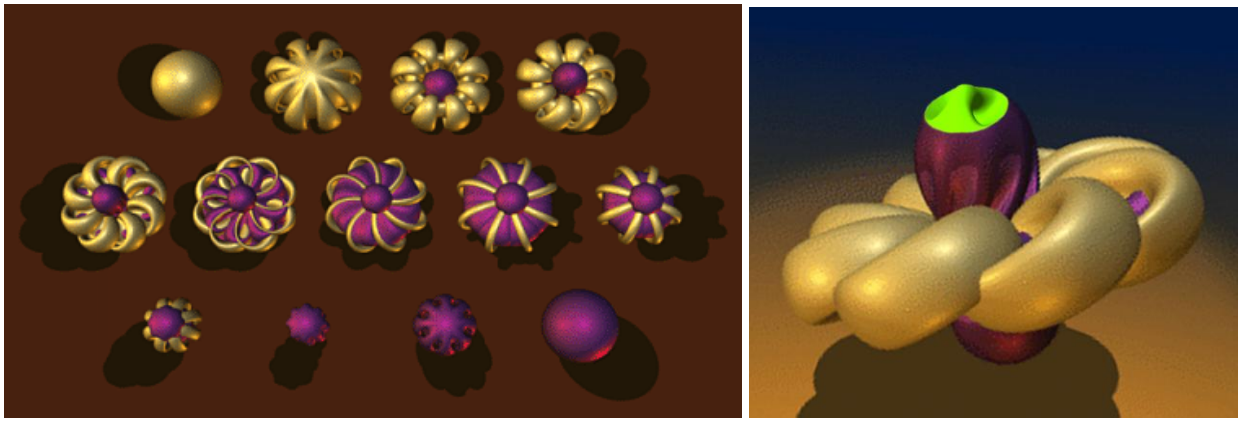

Figure 36: *(a) Overview of the "Outside-In" sphere eversion process [8]. (b) The disk carrying the geometry of the two intertwined torus tunnels riding on top of this eversion process.*

Looking for a More Direct Parameter-Swap Process

The above process seems rather lengthy and cumbersome. I would like to avoid having to go though separate, subsequent sphere-eversion and a torus-eversion processes. Thus, let's may try a brute-force approach:

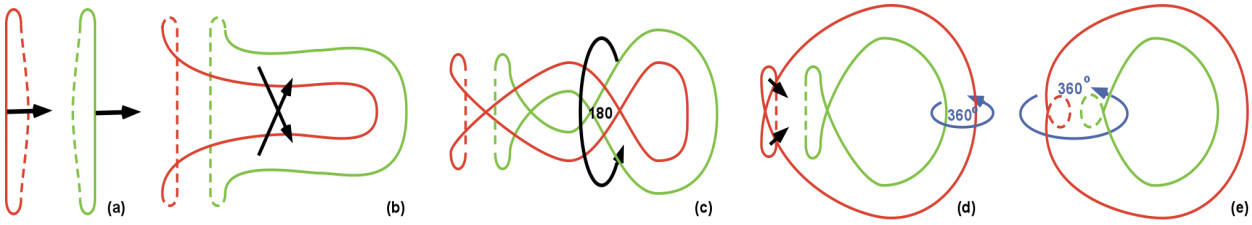

Figure 37: *Trying to force a parameter swap onto an ordinary torus of type* **OO**.

We start by stretching a standard torus into a tubular shape (Fig.37a) and then separate the outer sleeve from the inner one by moving it out to one side. This produces a rough new toroidal loop that shows the parameterization in the desired orientation (Fig.37b). Now we try to collapse the inner sleeve (shown with dashed lines) by moving the two Klein-bottle mouths towards each other. But in trying to let the two Klein-bottle mouths annihilate one another, two undesirable effects are observed. First, a crossover forms in the main toroidal loop (Fig.37c). This loop can be unwound with a UwSwXo-move, which, however, puts 360° of M-twist into this loop. Second, the collision of the two Klein-bottle mouths will not simply annihilate them via a triple fold (as in Fig.9e), since the two mouths are mirror images of one another. Instead they will form an internal collar in the toroidal tube (Fig.37d, 37e). Now we resort to the collar-unwinding process illustrated in Figures 23 and 24. As the collar loops unwind, the 360° M-twist in the torus tube is automatically consumed, leaving a pure torus of type **OO**.

Searching for the Energetically Least Expensive Transformation

Is the above process the best we can do? Ideally we are looking for some process, which we might call "Torus OptiSwap" that has the fewest topological events and/or the lowest maximum bending energy along the whole transformation sequence.

At this stage of my investigations I believe that some sort of sphere eversion process cannot be avoided to accomplish the parameter swap. Thus, if we are looking for a halfway point of lowest energy, then we probably should start with a more energy-efficient sphere eversion process, such as the "Optiverse" process [14]. We can easily implant our disk with the handle/tunnel geometry anywhere we want, for instance into one of the two crossing collar branches at the "top" of the Morin surface [10] . We would then again let the surface evolve towards lower energy states on either side of this half-way point. However, in one of the two states, the torus would still have to be subjected to a separate torus-eversion step to realize a pure parameter swap.

But I have even higher hopes for an efficient torus parameter swap! It should be possible to blend part of the handle/tunnel geometry into the Morin surface, so as to simplify the geometry and reduce the overall bending energy contained in this system. In principle we just need to accommodate one extra tunnel into the sphere eversion process. For instance, an extra tunnel could be inserted into one of the two crossing branches at the top of the Morin surface. We then keep track of that tunnel as we move through the whole sphere eversion process, and always find two circular regions, between which the tunnels is extended, that results in the energetically most favourable configuration.

But we then still have to do the separate torus eversion. The big challenge thus seems to avoid this step. In this light, the process in Figure 37 that goes through only one eversion process seems advantageous. Thus it seems worthwhile to look for the simplest way to remove such a collar – perhaps by distilling out the essence of the "Mexican Hat" move associated with Morin's sphere eversion process [10]. Again we may have to await the emergence of a surface optimization system that can properly account for twist and for any skew between the two sets of complementary parameter lines.

10. Conclusions

Four simple representatives for the four regular homotopy classes of the torus have been presented. They are easy to visualize and easy to remember. A rich set of regular homotopy-preserving transformations has been discussed. They should allow the reader to start from any arbitrary topological torus and readily identify its generic representative and into which class that torus belongs.

The effect of various possible changes to the parameterization of a torus has been clarified, and a complete map that shows how various tori classes transform into one another under such changes has been established (Fig.16). Explicit processes that perform some of these transformations have been described. In particular, it has been shown how the parameterization of an ordinary torus can be swapped by using some sphere-eversion process.

Work remains to be done to find the simplest, most elegant processes for some of the more important and intriguing transformations, in particular the torus eversion and the parameter swap processes. Work has begun on some special-purpose surface-optimization system that may allow us eventually to find some nice, stream-lined processes.

Acknowledgements

I would like to express my thanks to John Sullivan and to Matthias Goerner for stimulating discussions and various illuminating e-mail exchanges concerning *topology*, *homology*, *homotopy*, etc., and for a review of an early draft of this report. This work was supported in part by the National Science Foundation (NSF award #CMMI-1029662 (EDI)).

References

[1] K. Brakke, *Surface Evolver* – http://www.susqu.edu/brakke/evolver/evolver.html

[2] A. Cheritat, *The torus inside out*. – http://www.math.univ-toulouse.fr/~cheritat/lab/e_labo.html

[3] A. Cheritat, *Torus eversion: turing a torus inside out*. Video (49sec) – http://www.youtube.com/watch?v=kQcy5DvpvlM&feature=related

[4] *Dehn Twist*: – http://en.wikipedia.org/wiki/Dehn_twist

[5] G. K. Francis, *A Topological Picturebook*. Springer, New York. 1987. Chapter 7, Figs. 4 and 5.

[6] J. Hass and J. Hughes, *Immersions of Surfaces in 3-Manifolds*. Topology, Vol 24, No.1, pp 97-112, 1985.

[7] H.B. Lawson, *Complete minimal surfaces in* S^3, Ann. of Math., Vol. 92, pp. 335-374, 1970.

[8] S. Levy, D. Maxwell, D. Munzner, *Outside-In*. Video (22 min). – http://www.geom.uiuc.edu/docs/outreach/oi/

[9] N. L. Max, *Turning a Sphere Inside Out*. International Film Bureau, Chicago, 1977. Video (21 min); reissued by AK Peters, 2004. – http://www.akpeters.com/sphere

[10] B. Morin and J-P. Petit, *Le retournement de la sphère*. In *Les Progrès des Mathématiques*, pp 32-45. Pour la Science/Belin, Paris, 1980.

[11] A. Phillips, *Turning a Surface Inside Out*. Scientific American **214**, pp 112-120, Jan. 1966.

[12] K. Polthier, *Imaging math: Inside the Klein bottle*. -- http://plus.maths.org/issue26/features/mathart/index.html#LawsonKlein

Interactive applet: -- http://plus.maths.org/issue26/features/mathart/applets/appletLawsonKleinClipTop.html

[13] S. Smale, *A Classification of Immersions of the Two-Sphere*. Trans. Amer. Math. Soc. **90**, pp 281-290, 1958.

[14] J. M. Sullivan, G. Francis, and S. Levy. *The Optiverse*. In H-C. Hege and K. Polthier, eds, *VideoMath Festival at ICM'98*, Springer, 1998. Video (7 min).

[15] J. M. Sullivan, *A History of Sphere Eversions*. – http://torus.math.uiuc.edu/jms/Papers/isama/color/opt2.htm#fig4

[16] J. M. Sullivan, several private communications.

[17] H. Whitney, *Whitney umbrella*. – http://en.wikipedia.org/wiki/Whitney_umbrella